Behavioural Brain Research 427 (2022) 113868

Contents lists available at ScienceDirect

Behavioural Brain Research

journal homepage: www.elsevier.com/locate/bbr

Temporal dynamics of fMRI signal changes during conditioned interoceptive pain-related fear and safety acquisition and extinction

Franziska Labrenz [a,b,*], Tamás Spisák [c], Thomas M. Ernst [b], Carlos A. Gomes [d], Harald H. Quick [e,f], Nikolai Axmacher [d], Sigrid Elsenbruch [a,b], Dagmar Timmann [b]

[a] Department of Medical Psychology and Medical Sociology, Faculty of Medicine, Ruhr University Bochum, Bochum, Germany
[b] Department of Neurology, Center for Translational Neuro, and Behavioral Sciences (C-TNBS), University Hospital Essen, University of Duisburg-Essen, Essen, Germany
[c] Institute of Diagnostic and Interventional Radiology and Neuroradiology, University Hospital Essen, University of Duisburg-Essen, Essen, Germany
[d] Department of Neuropsychology, Institute of Cognitive Neuroscience, Faculty of Psychology, Ruhr University Bochum, Bochum, Germany
[e] High-Field and Hybrid Magnetic Resonance Imaging, University Hospital Essen, Essen, Germany
[f] Erwin L. Hahn Institute for MR Imaging, University of Duisburg-Essen, Essen, Germany

ARTICLE INFO

Keywords:
FMRI
Differential fear conditioning
Gut-brain axis
Pain-related fear
Safety learning
Temporal dynamics

ABSTRACT

Associative learning and memory mechanisms drive interoceptive signaling along the gut-brain axis, thus shaping affective-emotional reactions and behavior. Specifically, learning to predict potentially harmful, visceral pain is assumed to succeed within very few trials. However, the temporal dynamics of cerebellar and cerebral fMRI signal changes underlying early acquisition and extinction of learned fear signals and the concomitant evolvement of safety learning remain incompletely understood.

3 T fMRI data of healthy individuals from three studies were uniformly processed across the whole brain and the cerebellum. All studies employed differential delay conditioning (N = 94) with one visual cue (CS^+) being repeatedly paired with visceral pain as unconditioned stimulus (US) while a second cue remained unpaired (CS^-). During subsequent extinction (N = 51), all CS were presented without US.

Behavioral results revealed increased CS^+-aversiveness and CS^--pleasantness after conditioning and diminished valence ratings for both CS following extinction. During early acquisition, the CS^- induced linearly increasing neural activation in the insula, midcingulate cortex, hippocampus, precuneus as well as cerebral and cerebellar somatomotor regions. The comparison between acquisition and extinction phases yielded a CS^--induced linear increase in the posterior cingulate cortex and precuneus during early acquisition, while there was no evidence for linear fMRI signal changes for the CS^+ during acquisition and for both CS during extinction.

Based on theoretical accounts of discrimination and temporal difference learning, these results suggest a gradual evolvement of learned safety cues that engage emotional arousal, memory, and cortical modulatory networks. As safety signals are presumably more difficult to learn and to discriminate from learned threat cues, the underlying temporal dynamics may reflect enhanced salience and prediction processing as well as increasing demands for attentional resources and the integration of multisensory information. Maladaptive responses to learned safety signals are a clinically relevant phenotype in multiple conditions, including chronic visceral pain, and can be exceptionally resistant to modification or extinction. Through sustained hypervigilance, safety seeking constitutes one key component in pain and stress-related avoidance behavior, calling for future studies targeting the mechanisms of safety learning and extinction to advance current cognitive-behavioral treatment approaches.

1. Introduction

Translational research into the gut-brain axis has sparked tremendous interest in many fields of medicine as well as in the behavioral neurosciences. Along afferent and efferent pathways, signal transduction and processing between the gut and the brain are increasingly acknowledged to shape cognition, emotion and behavior [1,2]. While adaptive bidirectional interactions maintain the homeostatic state in

* Corresponding author at: Department of Medical Psychology and Medical Sociology, Faculty of Medicine, Ruhr University Bochum, Bochum, Germany.
E-mail address: franziska.labrenz@ruhr-uni-bochum.de (F. Labrenz).

https://doi.org/10.1016/j.bbr.2022.113868
Received 19 October 2021; Received in revised form 14 March 2022; Accepted 28 March 2022
Available online 29 March 2022

healthy organisms, dysfunction of the gut-brain axis contributes to altered affective and behavioral processes, with implications for multiple clinical conditions [3–6]. This complex interplay between the gut and the brain relies on interoception, which refers to the neuronal encoding, representation and integration of bodily signals, the impact of these signals on perceptions, cognitions and behaviors as well as the expression of these representations [7–9]. One major function of interoceptive signaling consists in affective-emotional experiences and memory [10,11], that are likely shaped by associative learning.

Associative learning is best accounted for by principles of Pavlovian conditioning principles, by which an initially neutral cue (conditioned stimulus; CS^+) is repeatedly paired with an aversive unconditioned stimulus (US). Upon presentation of the CS^+ alone, this stimulus evokes a response previously associated with the US, i.e., conditioned fear. In its application to the context of the gut-brain axis, conditioning with ecologically salient interoceptive US, like visceral pain, is capable of rapidly inducing interoceptive fear in response to the CS^+ in humans [12–14]. Moreover, learned fear was shown to foster hypervigilance and hyperalgesia in healthy volunteers [15–19] and in patients with chronic visceral pain [20–22]. In parallel, cues signaling the absence of an aversive interoceptive US, i.e., the CS^-, appear to become potent inhibitors of fear responses and as conditioned safety signals acquire rewarding properties [23]. These safety cues engage distinct neural activation patterns [24,25], with first evidence from the visceral pain field supporting separate neural mechanisms underlying fear and safety learning in the cerebrum [12,14] and cerebellum [21,26,27].

While traditional learning theories [28,29] assume that the associative strength between the CS and US aggregates over repeated trials, fear memories can also be rapidly formed and robustly maintained even after a single trial [30,31]. Aversive interoceptive perceptions, especially visceral pain, are highly salient, even when compared to exteroceptive pain. As such, interoceptive pain provides a conceptually valid US to study rapid and uniquely dynamic learning processes, and to investigate the time course of fear and safety acquisition and extinction. A first study utilizing visceral pain as US in a rapid conditioning procedure [32] demonstrated on the behavioral level successful differential learning with increased CS^+-aversiveness and CS^--pleasantness after acquisition and a return to baseline following rapid extinction. Although CS-US contingencies for the conditioned fear and safety signal were perceived as significantly different, the CS^--US contingency was highly overestimated suggesting that the predictive value of the safety cue was not fully established at the end of the rapid conditioning procedure. On a neural level, CS^+-induced activation patterns resembled the fear network reported for Pavlovian conditioning procedures in general [24] and visceral pain specifically [12–14,33]. For the safety signal, however, no changes in neural activation were evident during acquisition and extinction. Together with data on conditioned nausea [34] and taste aversion [35,36], interoceptive visceral pain may thus trigger a fundamental learning process and robust fear responses even after very few learning trials. However, studies addressing the time-dependent neural mechanisms underlying the initial learning and memory processes of pain-related fear and safety signals are scarce. Compared to commonly applied analyses of splitting acquisition and extinction into early, mid, and late phases, neuroimaging approaches to model putative linear and non-linear relationships in key brain regions of fear conditioning are a complex endeavor and have rarely been conducted in animals or humans. For example, amygdala activation is not consistently reported across different fear conditioning paradigms [24,37,38] supporting the assumption that amygdala responses adapt over time and might not be fully captured in analyses of mean activation across multiple trials [39]. However, results are mixed with some studies supporting this assumption [40,41], while others did not find time-dependent effects [42–44]. Therefore, more studies are needed utilizing linear and non-linear analyses of time-dependent neural mechanisms that might advance our understanding about the underlying time courses of key brain regions implicated in fear learning and extinction.

The aim of this analysis in a large combined dataset from healthy human conditioning studies was to explore the differences in the temporal dynamics of early fear and safety learning during acquisition and subsequent extinction in an experimental model of visceral pain. To do so, we conducted trial-by-trial analyses of the initial CS-US pairings, tested for linear changes in neural activation across these trials, and compared the activation patterns with averaged fMRI signal analyses as reported in previous neuroimaging studies.

2. Material and methods

2.1. Participants

For the purposes of this report, we combined and reanalyzed behavioral and 3 T fMRI data from three previously published conditioning studies [12,14,27], providing us with data from a combined sample of N = 94 healthy and young individuals (51 women and 43 men; mean age ± standard error of the mean (SEM) = 27.04 ± 0.86 years, mean body mass index (BMI) 23.62 ± 0.41 kg/m^2). These fMRI studies were conducted with highly standardized and parallelized procedures for recruitment, screening and data acquisition in the same biomedical research center with identical methodology for pain-related differential fear conditioning, as described in more detail below. These consistent study protocols enabled us to combine data from multiple studies in order to perform consolidated and quantitative analyses that require larger datasets. Thus, the results reported herein are novel and exceed the scope of the primary published analyses of the individual studies.

Recruitment and screening procedures were identical across studies with the following inclusion criteria: age 18 – 60 years, BMI 18 – 30 kg/m^2 and no medical and psychiatric conditions or chronic medication use except for hormonal contraceptives or occasional use of over-the-counter pain or allergy medications. All participants completed a comprehensive questionnaire battery for participant characterization including screening for anxiety and depression as well as ongoing gastrointestinal symptoms. A medical examination was conducted to exclude perianal tissue damage (e.g., painful hemorrhoids) potentially interfering with the experimental visceral pain model implemented in all studies (i.e., rectal distensions). All participants gave written informed consent and were reimbursed for their participation. All study protocols were approved by the local ethics committee of the University of Duisburg-Essen, (Germany) and followed the provisions of the Declaration of Helsinki.

2.2. Study designs and procedures

All studies implemented a differential delay conditioning paradigm using distinct visual stimuli as CS and visceral pain as US (for details see Table 1). The acquisition phase was identical for all studies, resulting in N = 94 data sets. For the extinction phase, N = 51 data sets were included for analyses herein. This exclusion of data was owed to distinct, study-specific protocols in primary studies, i.e., a test phase involving US [14] and a context change [12].

Prior to the experiment, all participants received identical instructions that the goal of the respective study was to investigate visceral pain-related learning and memory processes and that they would see visual stimuli and experience visceral pain without any information about CS-US contingencies. This approach demands participants to learn the associations between CS and US from trial to trial through predictions, which, in contrast to instructed learning where participants are informed about CS-US contingencies, does not depend on expectations raised through prior instructions.

During acquisition, one visual cue (CS^+) was repeatedly followed by a visceral pain stimulus (US; duration 14 – 16.8 s varying between studies) while a second cue (CS^-) was never followed by the US. For all studies, a total of 16 CS^+ and 16 CS^- were presented in pseudo-randomized order and with 75% reinforcement schedule, i.e., 12 CS^+

Table 1
Details on experimental designs and participants in primary studies.

	Acquisition			Extinction	
Study	N	CS	US	N	US
Icenhour et al. [12]	42 22 women 20 men	16 CS^+ 16 CS^- 8.0–12.0 s	12 US 14.0 s	21 11 women 10 men	6 CS^+ 6 CS^- 8.0–12.0 s
Kattoor et al. [13]	30 15 women 15 men	16 CS^+ 16 CS^- 7.2–12.0 s	12 US 16.8 s	30 15 women 15 men	12 CS^+ 12 CS^- 7.2–12.0 s
Labrenz et al. [14]	22 14 women 8 men	16 CS^+ 16 CS^- 6.0–12.0 s	12 US 16.8 s	–	–

Selected details on key aspects of experimental designs and participants are given for primary studies providing the data for the combined analyses presented herein. Given different combined Ns for acquisition and extinction phases, we show data separately for these different learning phases including the number and duration of the conditioned stimuli (CS) and unconditioned stimuli (US).

were followed by a US. Onset of the US varied randomly within all studies between 6 and 12 s after CS^+ onset and both stimuli co-terminated. The stimulus sequence for all studies started with two CS^+ presentations that were both reinforced followed by the first presentation of the CS^-. During extinction, a total of 12 CS (6 CS^+, 6 CS^-) [12] or 24 CS (12 CS^+, 12 CS^-) [27] were presented and never followed by a US. The stimulus sequence during extinction was the same order as in the acquisition phase starting with two CS^+ presentations followed by the first presentation of the CS^-. Inter-trial intervals (ITI) varied between 12 and 20 s.

Visceral pain as US in differential fear conditioning is a clinically relevant and well-established experimental model that has been validated in samples of healthy individuals [12–14,32,45] and patients with chronic visceral pain [20]. Visceral pain stimuli were applied using a pressure-controlled barostat system (modified ISOBAR 3 device, G & J Electronics, ON, Canada) and individually calibrated to ensure that participants would experience adequately painful stimuli during the experiment based on visual analog scale (VAS) ratings. Further details on the standardized calibration and thresholding procedures are given in the primary studies. Following a structural MRI scan, blood oxygen level dependent (BOLD) responses were acquired using event-related fMRI during consecutive phases of acquisition and extinction. All study protocols were accomplished within approximately 1.5 – 2 h on one day.

2.3. Measures and statistical analyses of behavioral data

At different time points during the conditioning procedure, online VAS ratings were presented to assess CS valence, CS-US contingencies and US painfulness using an MRI-compatible hand-held fiber optic response system (LUMItouchTM, Photon Control Inc., Burnaby, BC, Canada). Subjective reports in conditioning procedures provide valid and reliable outcome measures [46] and capture both affective ratings assessing changes in CS valence and cognitive ratings assessing awareness about the discrimination between CS-US associations. Based on our previous work, we could demonstrate that, as expected, CS^+-aversiveness and CS^--pleasantness increase after acquisition and return to baseline following extinction and that participants are aware about the CS-US contingencies during acquisition and extinction [12–14,47].

CS valence was assessed at baseline, after acquisition and after extinction by asking participants "How do you perceive the [symbol]?" on a VAS ranging from "− 100" indicating very pleasant to "+ 100" indicating very unpleasant and "0" indicating neutral. Following both acquisition and extinction, perceived CS-US contingency was assessed by asking participants "How often was the [symbol] followed by a rectal distention?" with endpoints "never" indicating 0% and "always" indicating 100%. Overall US painfulness was assessed after acquisition on a VAS ranging from "not painful at all" (0) to "very painful" (100).

Analyses of behavioral data were performed with the Statistical Package for the Social Sciences (IBM Corp. Released 2020. IBM SPSS Statistics for Windows, Version 27.0. Armonk, NY: IBM Corp). For statistical analyses of VAS CS valence ratings, a repeated measure analysis of variance (rm-ANOVA) was conducted with within subject factors CS type (CS^+, CS^-) and phase (baseline, acquisition, extinction). For the analyses of CS-US contingency, an rm-ANOVA with the within subject factors CS type (CS^+, CS^-) and phase (acquisition, extinction) was performed. Post-hoc t-tests were carried out for each CS separately using Bonferroni-correction to control for inflation of alpha (set at $p < .05$) and are reported with Cohen's d.

2.4. fMRI imaging and analysis

MR images for all studies were acquired on a 3 T whole-body MRI system (MAGNETOM Skyra, Siemens Healthcare GmbH, Erlangen, Germany) equipped either with a 32-channel head coil [12,14] or with 16 elements of a 20-channel head/neck DirectConnect coil [27]. Structural images were acquired using a three-dimensional T_1-weighted magnetization prepared rapid acquisition gradient echo (MPRAGE) sequence and BOLD contrast images were assessed with whole-brain functional MRI acquisition using echo-planar imaging (EPI) [27] or multi-echo EPI [12,14]. Details on the scanning parameters for each study are given in Table 2.

While the primary studies focused mainly on fMRI analyses utilizing region-of-interest analyses in a priori defined cerebral brain areas, the contribution of the cerebellum to pain-related differential learning and memory processes has rarely been addressed, except for one re-analysis [27]. However, the cerebellum is increasingly acknowledged to modulate processing in cortical and subcortical brain structures and to mediate fear learning [48–51]. By uniformly preprocessing the available raw data from the primary studies, we therefore aimed to create a large and homogeneous data set that allows investigating the cerebral and cerebellar mechanisms underlying pain-related fear and safety acquisition and extinction. All fMRI analyses were performed using SPM12 (Wellcome Department of Cognitive Neurology, London, UK; http://www.fil.ion.ucl.ac.uk/spm) implemented in Matlab 2019a. Functional images for each participant were corrected for slice timing and motion and normalized using the inverse deformation field and the individual warped bias corrected image that were previously segmented with the CAT12 toolbox implemented in SPM12 (http://www.neuro.uni-jena.de/cat/). Normalization of the cerebellum was performed using SUIT (http://www.diedrichsenlab.org/imaging/suit.htm). Images of the cerebrum were smoothed with an isotropic Gaussian kernel of 8 mm, while the smoothing kernel for cerebellar images had a FWHM of 4 mm.

First level analyses were carried out using a general linear model. Six realignment parameters for translation and rotation were included as multiple motion regressors to account for the rigid body transformation between each image and a reference image. A temporal high-pass filter with a cut-off period was set at 128 s. The time series of each voxel was fitted with a corresponding task regressor modeling a boxcar convolved with a canonical hemodynamic response function. The first level model for acquisition included a total of 15 regressors: the first six CS^+ and first six CS^- trials (one trial each), CS^+ and CS^- late acquisition (10 trials each) and US (12 trials; duration 14.0 s or 16.8 s). All CS events were set to a duration of 0 s. Equivalent regressors were modeled for extinction including six regressors for each of the initial CS trials (one trial each; zero duration).

To assess BOLD responses to pain-predictive (CS^+) and safety (CS^-) cues and the US during acquisition and extinction, we then computed first level contrasts for each phase and entered them into second level group analyses.

Table 2
Parameters of MRI scanning protocols.

		TR (ms)	TE (ms)	FA	FOV (mm)	Slice no.	Slice thick. (mm)	Voxel size (mm3)	Matrix (mm2)	GRAPPA
Icenhour et al. [12]	T_1	1900	2.13	9°	239	192	0.9	0.9 × 0.9 × 0.9	256 × 256	r = 2
	EPI	2000	13.0 28.9 44.8	90°	220	36	3.0	2.8 × 2.8 × 3.0	80 × 80	r = 3
Kattoor et al. [13]	T_1	1900	2.13	9°	239	192	0.9	0.9 × 0.9 × 0.9	256 × 256	r = 2
	EPI	2400	26	90°	240	42	3.0	2.6 × 2.6 × 3.0	94 × 94	r = 2
Labrenz et al. [14]	T_1	1900	2.13	9°	239	192	0.9	0.9 × 0.9 × 0.9	256 × 256	r = 2
	EPI	2000	13.0 28.9 44.8	90°	220	36	3.0	2.8 × 2.8 × 3.0	80 × 80	r = 3

Scanning parameters are given separately for the primary studies. Within each study, parameters were identical for the acquisition and extinction phases, including repetition time (TR), echo time (TE), flip angle (FA), number of slices (Slice no.), slice thickness (Slice thick.), voxel size, matrix size, all given with 100% phase resolution and the acceleration factor 'r' applied for parallel imaging using the Generalized Autocalibrating Partial Parallel Acquisition (GRAPPA).

Our first aim was to compare overall CS-induced neural activation patterns across early acquisition and extinction with results from previous neuroimaging studies implementing visceral pain-related fear conditioning [12–14,27,32] and with findings from previous meta-analyses [24,52]. To do so, the averaged BOLD response across the first six trials of each experimental phase was computed and on the second level compared against the implicit baseline: [CS^+ ACQ > Rest]; [CS^+ EXT > Rest]; [CS^- ACQ > Rest]; [CS^- EXT > Rest], and between experimental phases: [CS^+ ACQ vs. EXT]; [CS^- ACQ vs. EXT]. As a treatment check and to provide comparability with previous work assessing pain-related BOLD responses, we moreover computed a one sample t-test with [US > Rest] across the whole acquisition phase.

In a next step, we aimed to investigate the time course across the first trials of the acquisition and extinction phase in order to identify putative time-dependent changes in BOLD responses of the CS. Therefore, zero-mean linear contrast with increasing [− 2.5, − 1.5, − 0.5, 0.5, 1.5, 2.5] and decreasing [2.5, 1.5, 0.5, − 0.5, − 1.5, − 2.5] contrast weights were generated for each CS separately. These contrasts were tested on the group level for each experimental phase by means of one sample t-tests: [CS^+ ACQ increase]; [CS^+ ACQ decrease]; [CS^- ACQ increase]; [CS^- ACQ decrease]; [CS^+ EXT increase]; [CS^+ EXT decrease]; [CS^- EXT increase]; [CS^- EXT decrease], and between experimental phases by means of paired t-tests [CS^+ ACQ vs. EXT increase]; [CS^+ ACQ vs. EXT decrease]; [CS^- ACQ vs. EXT increase]; [CS^- ACQ vs. EXT decrease].

All analyses included study as covariate of no interest to account for possible biases in MRI data acquisition. Results are reported at the whole-brain level at $p < .05$ familywise error rate (FWE) based on Threshold-Free Cluster Enhancement (TFCE) statistics (http://neuro.uni-jena.de/tfce/; version 174 2019–01–07).

3. Results

3.1. Behavioral data

Behavioral data confirmed successful differential learning of predictive cue properties as indicated by a significant CS type x phase interaction for CS valence ($F = 81.28$, $p < .001$, $\eta^2 = .53$) (Fig. 1). This effect resulted from specific valence changes with significantly increased CS^+-aversiveness ($t = 12.76$, $p < 0.001$, $d = 1.31$) and CS^--pleasantness ($t = 5.13$, $p < .001$, $d = 0.53$) from baseline to acquisition and a relative return to baseline after extinction for both CS^+ ($t = 4.82$, $p < .001$, $d = 0.57$) and CS^- ($t = 8.13$, $p < .001$, $d = 0.95$). Analysis of CS-US contingency also revealed an interaction effect ($F = 116.10$, $p < .001$, $\eta^2 = 0.62$) with a significantly higher perceived contingency for CS^+-US pairings compared to the CS^- after acquisition ($t = 14.43$, $p < .001$, $d = 1.48$) that diminished after extinction but still remained significant ($t = 2.40$, $p = .038$, $d = 0.28$).

In line with the primary studies, US intensity after acquisition was rated with 72.47 ± 1.66 mm indicating that participants perceived the visceral pain stimulus applied during acquisition as painful.

3.2. fMRI data

3.2.1. Averaged BOLD responses during early acquisition and extinction

Findings of CS-induced BOLD responses during early acquisition and early extinction are summarized in Tables 3 and 4, respectively. During early acquisition, enhanced CS^+-related activation (Fig. 2A) was observed in the inferior, middle, and superior frontal gyrus, lateral orbital gyrus, anterior insula, midcingulate cortex, inferior and superior

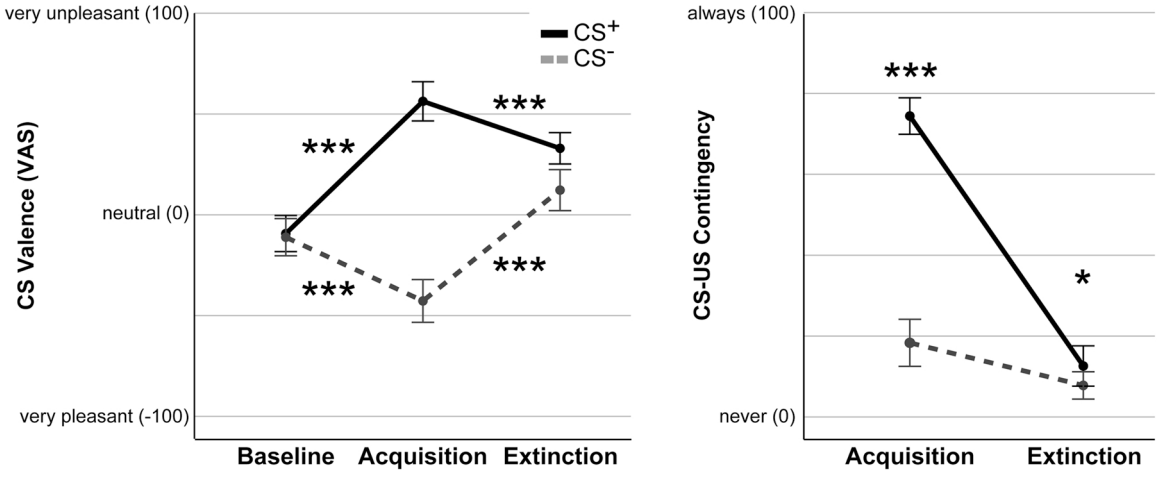

Fig. 1. Behavioral data on CS valence (left panel) and CS-US contingency (right panel) assessed with visual analogue scales (VAS) at baseline, after acquisition and after extinction. Data are shown as mean ± standard error of the mean. *** p < . 001, * p < .05.

Table 3
Averaged BOLD responses during early acquisition.

Location	k_E	x	y	z	TFCE	p_{FWE}	Network
CS^+ > Rest							
Inferior occipital gyrus	151985	24	-87	-1	32262.06	< 0.001	Visual
Middle occipital gyrus		31	-89	3	31318.52	< 0.001	Visual
Supramarginal gyrus	20218	-55	-50	38	9981.37	< 0.001	Default
Superior parietal lobule		-48	-51	63	8836.55	< 0.001	Fronto-parietal
Angular gyrus		-44	-55	56	8536.84	< 0.001	Fronto-parietal
Inferior frontal gyrus tri.	97509	53	22	0	8860.08	< 0.001	Default
Inferior frontal gyrus oper.		52	19	3	8833.71	< 0.010	Fronto-parietal
Inferior frontal gyrus orb.		44	25	-15	8764.26	< 0.001	Default
Anterior insula		45	21	-7	8744.34	< 0.001	Default
Middle frontal gyrus		45	10	48	8609.71	< 0.001	Fronto-parietal
Superior frontal gyrus		27	55	15	7883.24	< 0.001	Fronto-parietal
Angular gyrus	33610	50	-56	54	7856.83	< 0.001	Fronto-parietal
Supramarginal gyrus		54	-42	32	7818.88	< 0.001	Default
Superior parietal lobule		41	-56	56	7645.28	< 0.001	Fronto-parietal
Middle frontal gyrus	50542	-32	50	26	6804.67	.001	Ventral attention
Inferior frontal gyrus orb.		-39	54	-3	6380.20	.001	Fronto-parietal
Lateral orbital gyrus		-43	50	-10	6127.64	.001	Default
Thalamus	421	-9	-3	0	2937.95	.041	–
Pallidum		-13	4	-1	2854.00	.045	–
Midcingulate cortex	215	1	-21	30	2912.53	.043	Fronto-parietal
Putamen	1	26	13	10	2843.02	.047	–
Middle temporal gyrus	1	72	-26	-16	2824.65	.048	Fronto-parietal
Cerebellar Crus I	36420	-27	-79	-21	4788.96	< 0.001	Fronto-parietal
Cerebellar lobule VI		-32	-62	-30	4138.28	< 0.001	Fronto-parietal
Cerebellar Crus II		-16	-74	-37	3533.32	< 0.001	Fronto-parietal
Cerebellar Crus I		32	-77	-20	3354.09	< 0.001	Default
Cerebellar lobule VI		29	-72	-18	3029.58	< 0.001	Visual
Cerebellar lobule X	183	-16	-37	-46	808.47	.042	Fronto-parietal
Cerebellar lobule IX	51	-7	-56	-43	779.51	.046	Default
CS^- > Rest							
Fusiform gyrus	740798	-25	-85	-18	53652.82	< 0.001	Visual
Inferior occipital gyrus		-26	-91	0	52561.46	< 0.001	Visual
Angular gyrus	23	57	-68	44	4100.89	.009	Default
Angular gyrus	1	-41	-54	22	3219.50	.024	Default
Postcentral gyrus	318	53	-13	66	2904.27	.035	Somatomotor
Inferior frontal gyrus oper.	1	-63	3	11	2825.15	.038	Ventral attention
Middle frontal gyrus	1	-31	-20	36	2825.15	.038	Somatomotor
Superior frontal gyrus	2	-23	65	0	2825.15	.038	Default
Gyrus rectus	1	1	47	-26	2825.15	.038	Limbic
Anterior cingulate cortex	1	16	34	22	2825.15	.038	Fronto-parietal
Midcingulate cortex	1	-8	21	36	2825.15	.038	Ventral attention
Midcingulate cortex	5	13	18	29	2825.15	.038	Ventral attention
Posterior insula	1	-38	-7	2	2825.15	.038	Ventral attention
Posterior insula	1	36	-15	0	2825.62	.038	Ventral attention
Precentral gyrus	1	-43	6	40	2825.15	.038	Fronto-parietal
Precentral gyrus	1	39	-23	59	2825.15	.038	Somatomotor
Postcentral gyrus	1	-64	-9	28	2825.15	.038	Somatomotor
Parahippocampal gyrus	1	24	0	-34	2825.97	.038	Limbic
Rolandic operculum	1	37	-27	21	2825.15	.038	Somatomotor
Middle temporal gyrus	1	-66	-21	-24	2825.15	.038	Default
Middle temporal gyrus	5	63	-21	-14	2825.15	.038	Default
Superior temporal gyrus	1	-66	-45	19	2825.62	.038	Ventral attention
Temporal pole	1	58	8	-24	2825.15	.038	Default
Supramarginal gyrus	1	68	-27	22	2825.15	.038	Ventral attention
Caudate nucleus	2	-16	-1	21	2825.15	.038	–
Caudate nucleus	1	13	22	-5	2825.15	.038	–
Cerebellar Crus I	59628	-27	-82	-22	6684.60	< 0.001	Default
Cerebellar lobule VI		-28	-71	-24	6564.62	< 0.001	Fronto-parietal
Cerebellar lobule I-IV	215	-10	-38	-22	814.30	.036	Somatomotor
Cerebellar lobule I-IV		-8	-46	-26	752.11	.048	Limbic

Results of one sample t-tests assessing CS-induced BOLD responses against rest across the first six trials of the acquisition phase. Peak activations in the cerebrum are given with MNI coordinates and the corresponding large-scale network according to [124]. Peak activations in the cerebellum are given with SUIT coordinates and the corresponding large-scale network according to [123]. Activation clusters are reported with cluster size kE after application of Threshold-Free Cluster Enhancement (TFCE) at $p < .05$ familywise error (FWE) correction. Abbreviations: tri., triangularis; oper., opercularis; orb., orbitalis.

parietal lobule, pallidum, putamen, and thalamus. Cerebellar peak activations encompassed clusters in Crus I, Crus II, and lobules VI, IX, and X. Analyses of the CS^- (Fig. 2B) yielded increased BOLD responses mainly in the primary somatosensory cortex and additionally in small clusters encompassing the inferior, middle, and superior frontal gyrus, gyrus rectus, anterior and midcingulate cortex, posterior insula, parahippocampal gyrus, Rolandic operculum, inferior parietal lobule, temporal lobe, and caudate nucleus. Clusters in the cerebellum showing increased CS^--related responses involved Crus I, lobule I-IV, and lobule VI.

During extinction, enhanced CS^+-induced activation (Fig. 2C) was observed in the inferior parietal lobule as well as in cerebellar Crus I and II, lobule VIIb, VIIIb, and VI. In contrast, analysis of the CS^- (Fig. 2D) revealed a stronger involvement of the inferior and middle frontal gyrus

Table 4
Averaged BOLD responses during early extinction.

Location	k_E	x	y	z	TFCE	p_{FWE}	Network
CS^+ > Rest							
Middle occipital gyrus	49346	-25	-93	1	5546.86	.001	Visual
Inferior occipital gyrus		-27	-92	-10	5410.00	.002	Visual
Angular gyrus	3366	54	-51	50	3237.19	.021	Fronto-parietal
Supramarginal gyrus		51	-46	56	2896.35	.033	Fronto-parietal
Cerebellar Crus I	12479	-26	-74	-28	1814.64	< 0.001	Default
Cerebellar Crus I		-33	-69	-26	1740.32	.001	Fronto-parietal
Cerebellar lobule VIIb		-19	-75	-48	1398.94	.002	Ventral attention
Cerebellar Crus II		-14	-79	-39	1341.91	.003	Default
Cerebellar Crus II	1365	21	-78	-48	965.00	.023	Fronto-parietal
Cerebellar Crus II		33	-76	-44	910.01	.028	Default
Cerebellar lobule VIIb	217	39	-67	-59	919.16	.027	Fronto-parietal
Cerebellar Crus I	1522	9	-78	-29	913.36	.028	Fronto-parietal
Cerebellar Crus I		21	-82	-21	892.94	.030	Default
Cerebellar lobule VI	45	-17	-71	-18	797.87	.046	Ventral attention
CS^- > Rest							
Middle occipital gyrus	30357	-28	-96	-2	4999.54	.003	Visual
Inferior occipital gyrus		-23	-90	-11	4432.98	.005	Visual
Middle frontal gyrus	847	-43	48	13	3327.12	.024	Fronto-parietal
Inferior frontal gyrus tri.		-49	48	7	3082.41	.034	Fronto-parietal
Middle frontal gyrus	378	46	50	5	2984.10	.038	Fronto-parietal

Results of one sample t-tests assessing CS-induced BOLD responses against rest across the first six trials of the extinction phase. Peak activations in the cerebrum are given with MNI coordinates and the corresponding large-scale network according to [124]. Peak activations in the cerebellum are given with SUIT coordinates and the corresponding large-scale network according to [123]. Activation clusters are reported with cluster size kE after application of Threshold-Free Cluster Enhancement (TFCE) at $p < .05$ familywise error (FWE) correction.

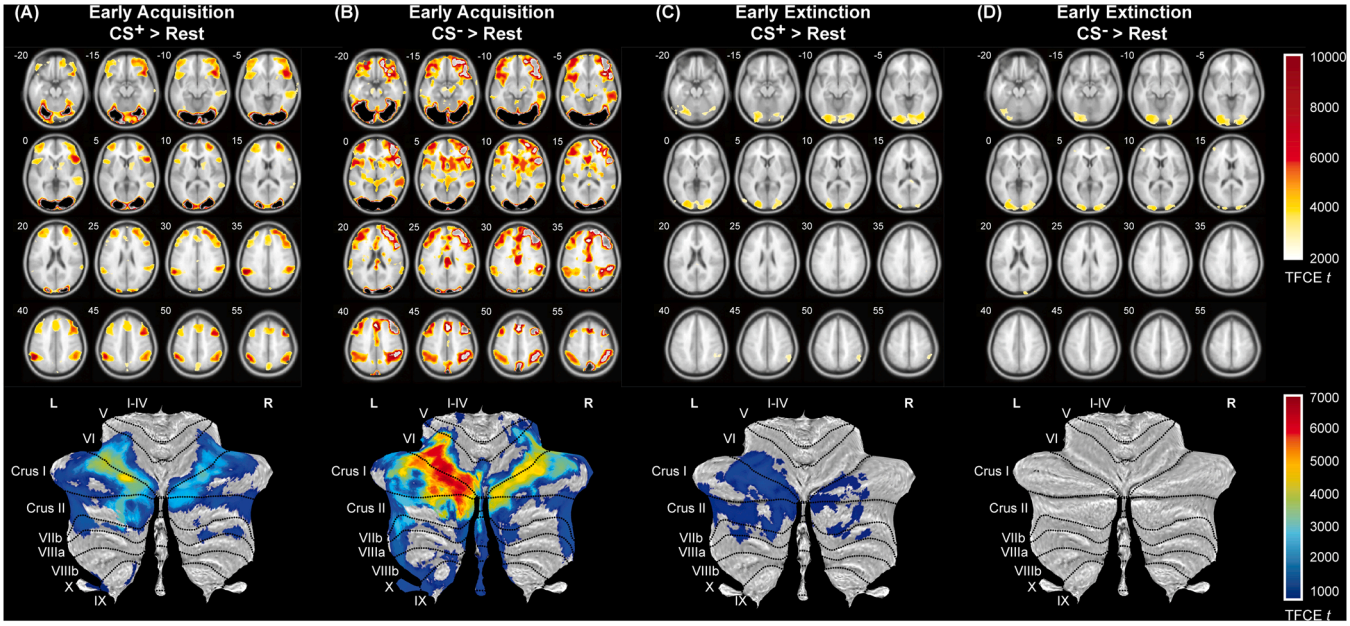

Fig. 2. CS-induced averaged BOLD responses during early acquisition and extinction displayed separately for the cerebrum (upper panel) and cerebellum (lower panel). Analyses of one sample t-tests yielded for the CS^+ during acquisition **(A)** significant clusters in inferior, middle, and superior frontal gyrus, lateral orbital gyrus, anterior insula, midcingulate cortex, inferior and superior parietal lobule, pallidum, thalamus, cerebellar Crus I, Crus II, lobules VI, X, and IX. Enhanced CS^--induced activation during acquisition **(B)** was found in angular and postcentral gyrus as well as cerebellar Crus I, lobules I-IV and VI. For the CS^+ during extinction **(C)**, enhanced neural activation was observed in angular and supramarginal gyrus as well as cerebellar Crus I, Crus II, lobules VI and VIIb. For the CS^- **(D)** increased neural activation was found in inferior and middle frontal gyrus. Significant clusters in the cerebellum are based on the SUIT atlas introduced by [122] and are displayed on a surface-based flatmap of the cerebellum (http://www.diedrichsenlab.org/imaging/suit_flatmap.htm). Activations indicated in black exceed the respective TFCE t threshold. All activation clusters are displayed at $p < .05$ familywise error rate (FWE) correction based on the Threshold-Free Cluster Enhancement (TFCE) statistic image.

while no cerebellar clusters emerged.

Analyses of differential responses comparing CS-related activation between experimental phases demonstrated enhanced BOLD responses during early extinction compared to early acquisition only for the CS^+ in the precuneus ($k_E = 141$; MNI coordinates $x = 3$, $y = -60$, $z = 20$, TFCE $t = 2451.84$, $p = .047$), which corresponds to the default mode network. However, no differential responses were evident in the reverse contrast or for analyses of the CS^-.

Analysis of neural responses induced by the visceral pain US (Table 5, Fig. 3) across the whole acquisition phase revealed a widespread network including the inferior, middle, and superior frontal gyrus, lateral orbital gyrus, anterior insula, precentral gyrus, inferior

Table 5
Distension-induced neural activation.

Location	k_E	x	y	z	TFCE	p_{FWE}	Network
Anterior insula	113651	37	7	9	21766.94	< 0.001	Ventral attention
Inferior frontal gyrus oper.		53	10	6	20610.40	< 0.001	Ventral attention
Putamen		26	9	6	13924.36	< 0.001	–
Precentral gyrus		-56	6	3	13605.86	< 0.001	Ventral attention
Pallidum		16	5	0	13560.32	< 0.001	–
Thalamus		8	-5	0	12881.24	< 0.001	–
Supramarginal gyrus	26214	50	-26	26	15592.75	< 0.001	Ventral attention
Angular gyrus		53	-51	53	10786.88	< 0.001	Fronto-parietal
Middle occipital gyrus	71130	28	-100	-1	12941.54	< 0.001	Visual
Calcarine cortex		-8	-95	-5	12514.47	< 0.001	Visual
Supramarginal gyrus	13087	-63	-37	35	10873.77	< 0.001	Ventral attention
Angular gyrus		-55	-55	45	4533.97	.005	Default
Middle frontal gyrus	7436	38	46	35	4175.85	.009	Ventral attention
Inferior frontal gyrus tri.		44	44	3	3722.05	.014	Fronto-parietal
Superior frontal gyrus		31	57	26	3225.56	.029	Fronto-parietal
Lateral orbital gyrus		40	59	-12	3165.04	.032	Fronto-parietal
Cerebellar lobule VI	26300	-30	-64	-26	6618.08	< 0.001	Fronto-parietal
Cerebellar lobule VI		-32	-56	-27	6592.89	< 0.001	Ventral attention
Cerebellar Crus I		-30	-72	-25	5657.57	< 0.001	Fronto-parietal
Cerebellar Crus I		-25	-80	-24	2704.25	< 0.001	Default
Cerebellar Vermis IX		1	-54	-33	2516.22	.001	Default
Cerebellar lobule VIIIa		-21	-65	-45	2490.98	.001	Ventral attention
Cerebellar lobule VIIb		-18	-71	-44	2256.24	.001	Ventral attention
Cerebellar Crus II		-31	-71	-42	2135.22	.001	Fronto-parietal
Cerebellar lobule I-IV		0	-50	-20	1681.69	.003	Somatomotor
Cerebellar lobule VI	9716	30	-62	-24	2310.62	.001	Ventral attention
Cerebellar lobule VI		34	-44	-39	2061.28	.001	Fronto-parietal
Cerebellar Crus I		35	-70	-27	2021.54	.001	Fronto-parietal
Cerebellar lobule I-IV		27	-33	-35	1901.93	.002	Limbic
Cerebellar lobule V		29	-35	-32	1897.20	.002	Somatomotor
Cerebellar lobule X		27	-38	-42	1614.51	.003	Dorsal attention
Cerebellar lobule VIIb		37	-47	-49	1135.05	.016	Ventral attention
Cerebellar lobule VIIIa		34	-43	-46	1132.02	.016	Ventral attention
Cerebellar Crus II		32	-68	-40	946.94	.031	Default
Cerebellar lobule VIIb	338	19	-69	-46	1053.93	.021	Dorsal attention

Results of the sample t-test assessing US-induced neural activation across the whole acquisition phase by means of the averaged BOLD response contrasted against rest. Peak activations in the cerebrum are given with MNI coordinates and the corresponding large-scale network according to [124]. Peak activations in the cerebellum are given with SUIT coordinates and the corresponding large-scale network according to [123]. Activation clusters are reported with cluster size kE after application of Threshold-Free Cluster Enhancement (TFCE) at $p < .05$ familywise error (FWE) correction.

parietal lobule, pallidum, putamen, and thalamus. Cerebellar activation clusters encompassed Crus I and II, lobules I-IV, V, VI, VIIb, and VIIIa, X as well as Vermis IX.

3.2.2. Temporal dynamics of BOLD responses during early acquisition and extinction

Results of CS-induced increases in BOLD responses during early acquisition and early extinction are summarized in Table 6. During early acquisition, a linear increase in BOLD responses was observed only in response to the CS^- (Fig. 4) with clusters encompassing mainly the anterior and posterior insula, midcingulate cortex, paracentral lobule, supplementary motor cortex, angular gyrus, precuneus, and hippocampus as well as small clusters encompassing the superior frontal gyrus, precentral and postcentral gyrus, Rolandic operculum, superior parietal lobule, pallidum, putamen, and thalamus. Increases in cerebellar BOLD responses were found in lobules I-IV, V, and VI. (Table 7). During early extinction, analyses of linear contrasts revealed no significant increase or decrease in BOLD responses for either CS.

Finally, analyses comparing the trial-by-trial changes in BOLD responses between the experimental phases revealed an increase in neural activation in response to the CS^- during early acquisition compared to early extinction in the posterior cingulate cortex and precuneus without any contribution of the cerebellum. In the reverse contrast as well as for the CS^+, analyses yielded no significant differential activation.

4. Discussion

The ability to predict potentially harmful signals arising from the gut is an evolutionary preserved learning process aiming at self-protection and survival. The immediate association of interoceptive signals with environmental cues is therefore assumed to succeed within very few trials, as demonstrated in experimental settings investigating visceral pain-related fear conditioning, extinction, and reinstatement [32], conditioned nausea [34] and taste aversion [35,36]. In the presence of such highly aversive events, cues signaling the absence of imminent pain acquire characteristics of relief, reward, and safety and act as potent inhibitors of fear [23]. However, as successful safety learning relies on a consolidated association between a threat cue and the aversive US, the underlying time courses of fear and safety learning presumably diverge. Therefore, we aimed to confirm and extend previous work addressing the neural mechanisms engaged during visceral pain-related learning and memory processes in a large combined sample. Previous analyses have mainly relied on the averaged neural activation across learning phases, implicating that human fear-conditioning experiments evoke consistent BOLD responses to conditioned stimuli. In line with theoretical models of learning [28], however, accumulating evidence demonstrates the relevance of transient responses during fear learning and extinction that are capable to depict the temporally graded evolvement of conditioned responses [53]. Therefore, our second aim was to identify the time-dependent neural responses to conditioned threat and safety signals during early phases of visceral pain-related acquisition and extinction.

Behavioral evaluations of differential fear conditioning are commonly assessed using subjective ratings of CS valence that contrast emotional states of aversiveness with states of pleasantness [46,54,55]. Utilizing visceral pain as US, contingent CS-US pairings consistently

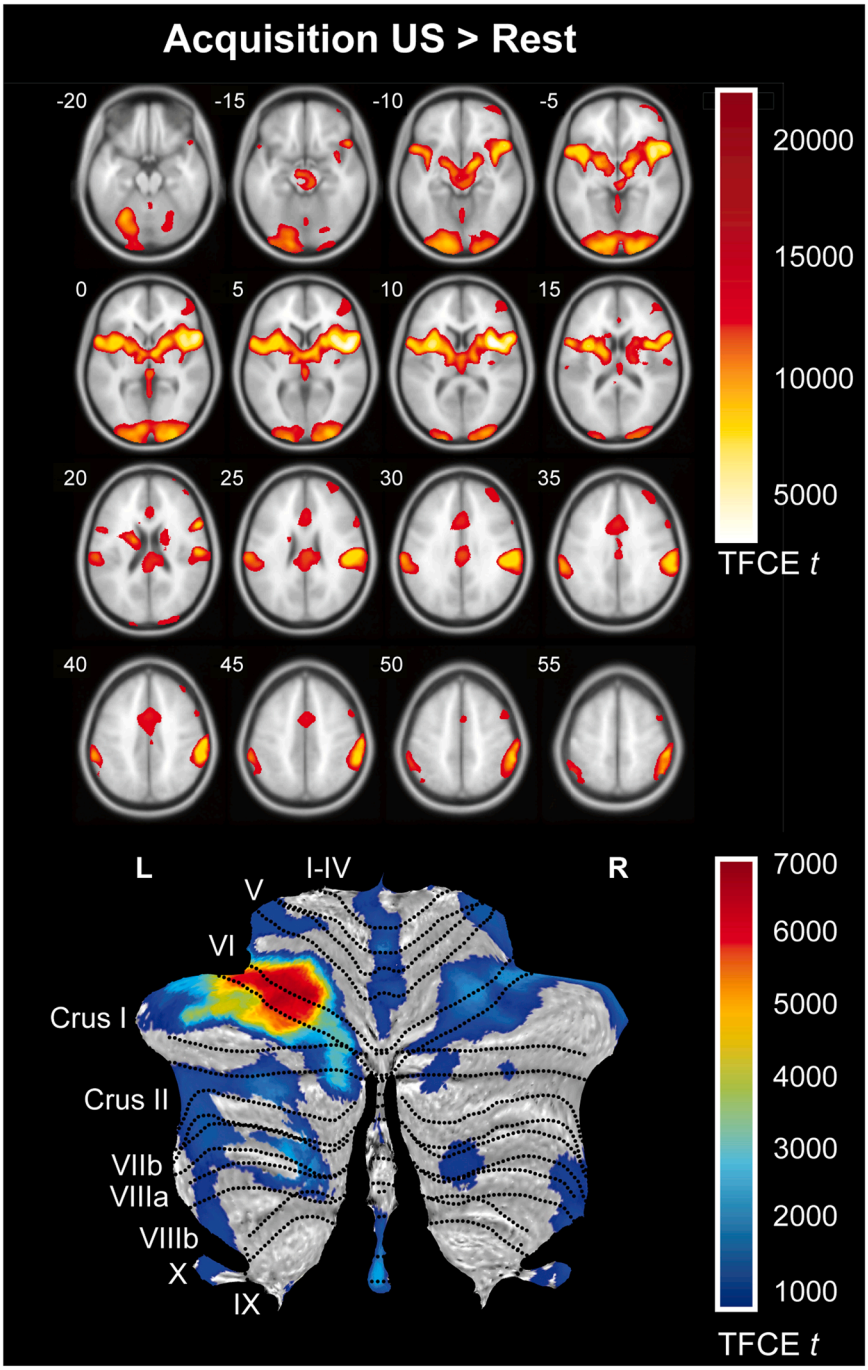

Fig. 3. US-induced neural activation during the whole acquisition phase. Increased neural activation was observed in inferior, middle, and superior frontal gyrus, lateral orbital gyrus, precentral gyrus, anterior insula, inferior parietal lobule, pallidum, and putamen. Cerebellar clusters encompassed Crus I and II as well as lobules I-IV, VI, V, IX, X, VIIb, and VIIIa. Significant clusters in the cerebellum are based on the SUIT atlas introduced by [122] and the 7-network parcellation [123] and are displayed on a surface-based flatmap of the cerebellum (http://www.diedrichsenlab.org/imaging/suit_flatmap.htm). All activation clusters are displayed at $p < .05$ familywise error rate (FWE) correction based on the Threshold-Free Cluster Enhancement (TFCE) statistic image.

induced an increase in negative emotional valence of the threat cue while cues signaling the absence of pain were increasingly reported as pleasant [12–14,32,56]. Our behavioral results from the combined sample confirmed these findings, accompanied by accurate CS-US contingency ratings and high aversiveness of the visceral pain stimulus. After repeated exposure to the conditioned stimuli without presentation of the US, CS valence and CS-US contingency ratings expectedly diminished demonstrating successful extinction. In line with the fMRI trial-by-trial analysis approach, respective behavioral data derived from intermittent ratings would have been beneficial in providing a more detailed insight into the underlying learning dynamics. However, the time points for the assessment of subjective learning measures need to be carefully balanced between methodological considerations and the study aim. For instance, including ratings of CS valence and CS-US contingencies during the experimental phases may interfere with the learning process, e.g., by creating contingency awareness and triggering other memory processes that in turn may affect the strength of the developing conditioned response [46].

In line with previous work elucidating the brain mechanisms involved in the generation of conditioned emotional responses [24,57], our results of the averaged neural activation confirmed the involvement of consistently evoked large-scale, yet distinct brain networks mediating visceral pain-related fear and safety learning. During early acquisition, the threat cue recruited a widespread network of fronto-parietal areas, anterior insula, midcingulate cortex, pallidum, and thalamus as well as cerebellar Crus I, Crus II and lobules VI, IX, and X which correspond to the fronto-parietal, default and visual network. For the safety cue, we observed increased neural activation in prefrontal and somatomotor

Table 6
Trial-by-trial changes in BOLD responses during early acquisition.

Location	k_E	x	y	z	TFCE	p_{FWE}	Network
CS^+ linear increase	No significant results						
CS^+ linear decrease	No significant results						
CS^- linear increase							
Parahippocampal gyrus	5116	-31	-38	-9	3560.43	.017	Visual
Lingual gyrus		-25	-44	-9	3444.40	.020	Visual
Fusiform gyrus		-24	-47	-17	3244.62	.025	Visual
Middle occipital gyrus	5637	-38	-85	28	3473.16	.019	Dorsal attention
Middle occipital gyrus	3668	44	-76	24	3245.63	.025	Dorsal attention
Middle temporal gyrus		41	-69	21	3200.45	.027	Dorsal attention
Angular gyrus		43	-75	33	3031.59	.031	Fronto-parietal
Supplementary motor area	9346	13	1	45	3147.80	.029	Somatomotor
Midcingulate cortex		13	-10	44	3105.90	.030	Somatomotor
Supplementary motor area		-2	-13	57	3088.31	.030	Somatomotor
Anterior insula	7365	43	0	16	3131.84	.029	Somatomotor
Posterior insula		37	-6	15	3100.85	.030	Somatomotor
Precuneus	9278	24	-55	27	3052.79	.031	Visual
Superior occipital gyrus		21	-71	29	3038.01	.031	Visual
Cuneus		19	-58	20	3014.29	.033	Default
Hippocampus	503	32	-26	-13	2860.17	.041	–
Paracentral lobule	887	9	-35	57	2844.20	.042	Somatomotor
Inferior temporal gyrus	293	49	-46	-8	2776.61	.046	Dorsal attention
Middle temporal gyrus		52	-53	-2	2730.15	.049	Dorsal attention
Superior frontal gyrus	1	22	-10	59	2836.86	.042	Dorsal attention
Putamen	1	29	6	4	2774.72	.046	–
Rolandic operculum	1	42	-20	18	2774.72	.046	Somatomotor
Superior parietal lobule	1	20	-58	54	2773.11	.046	Visual
Precentral gyrus	2	20	-20	64	2772.21	.046	Somatomotor
Precentral gyrus	1	-20	-18	59	2772.21	.046	Somatomotor
Postcentral gyrus	1	25	-39	60	2740.13	.049	Somatomotor
Pallidum	1	22	-1	-2	2746.77	.048	–
Thalamus	1	19	-15	2	2746.77	.048	–
Cerebellar lobule I-IV	596	2	-44	-14	892.83	.018	Somatomotor
Cerebellar lobule I-IV		-4	-50	-21	804.10	.031	Limbic
Cerebellar lobule VI	302	-18	-56	-26	803.16	.031	Somatomotor
Cerebellar lobule V		-18	-52	-15	739.63	.044	Somatomotor
Cerebellar lobule V		-14	-50	-22	729.84	.045	Somatomotor
CS^- linear decrease	No significant results						

Results of one sample t-tests assessing CS-induced neural activation across the first six trials of the acquisition phase by means of zero-mean linear increases and decreases in BOLD responses. Peak activations in the cerebrum are given with MNI coordinates and the corresponding large-scale network according to [124]. Peak activations in the cerebellum are given with SUIT coordinates and the corresponding large-scale network according to [123]. Activation clusters are reported with cluster size kE after application of Threshold-Free Cluster Enhancement (TFCE) at $p < .05$ familywise error (FWE) correction.

areas, anterior and midcingulate cortex, posterior insula, inferior parietal lobule, and caudate nucleus with additional cerebellar engagement of Crus I, lobules I-IV and VI. Together, these results extend knowledge about the involvement of specially the dorsolateral prefrontal cortex (PFC), anterior insula, ventral striatum, and thalamus during pain-related fear learning, while learning about cues signaling the absence of pain engages anterior and ventromedial parts of the PFC and brain regions implicated in somatosensory processing. The pattern of cerebellar activations are in very good agreement with previous fMRI studies on fear learning using aversive somatic stimulation [52,58], and provide further evidence that the cerebellum is part of the neurocircuitry for fear and anxiety [59]. Moreover, in contrast to the cerebral activation patterns, cerebellar regions identified during initial fear and safety learning were largely identical, in line with studies emphasizing that the role of the cerebellum goes far beyond motor learning and performance, and includes a contribution to various cognitive and emotional functions [60,61]. During extinction, threat-related brain responses were observed in the inferior parietal lobule, cerebellar Crus I, Crus II, lobule VI and VIIb, while safety learning engaged the ventrolateral and dorsolateral PFC. Overall, cerebral brain responses were diminished for both cues during extinction compared to acquisition. The inferior parietal lobule serves as a hub to integrate cross-modal information and is involved in focused attention as well as the allocation and reorientation of attention to relevant information through bottom-up pathways [62]. The ventrolateral PFC is of pivotal importance in the regulation of attention and emotion [63–67], including the evaluation and regulation of threat-related stimuli [68]. Likewise, the dorsolateral PFC is associated with conscious threat appraisal [69,70], working memory and attentional processes [71]. As CS-US contingencies have changed for the threat cue during extinction that now also signals the absence of pain, increased attentional resources may be necessary to govern putative changes for the safety cue. Moreover, the fear response is assumed to gradually decrease, thereby initiating a re-evaluation of the safety cue that is no longer required to inhibit the fear response. Taken together, the herein identified brain networks during early acquisition and partially also during early extinction substantiate previous findings, implicating the relevance of fronto-parietal areas, anterior insula, basal ganglia, and thalamus as well as cerebellar regions mediating cognitive-emotional aspects in associative learning and memory processes. However, the dynamic changes within these networks and the putative differences in the temporal evolvement of conditioned threat and safety cues have rarely been investigated. As visceral pain-related conditioning is assumed to occur rapidly [32], possibly due to the high salience of visceral pain compared to other modalities [45,56], this model might be ideally suited to investigate the temporal dynamics underlying fear and safety learning.

Approaches to model time-dependent neural mechanisms complement commonly applied analyses of splitting acquisition and extinction into early, mid, and late phases, and may advance knowledge about the dynamic temporal changes in key brain regions implicated in pain-related fear learning and extinction. Utilizing trial-by-trial analyses, we found gradually increasing neural activation during initial safety

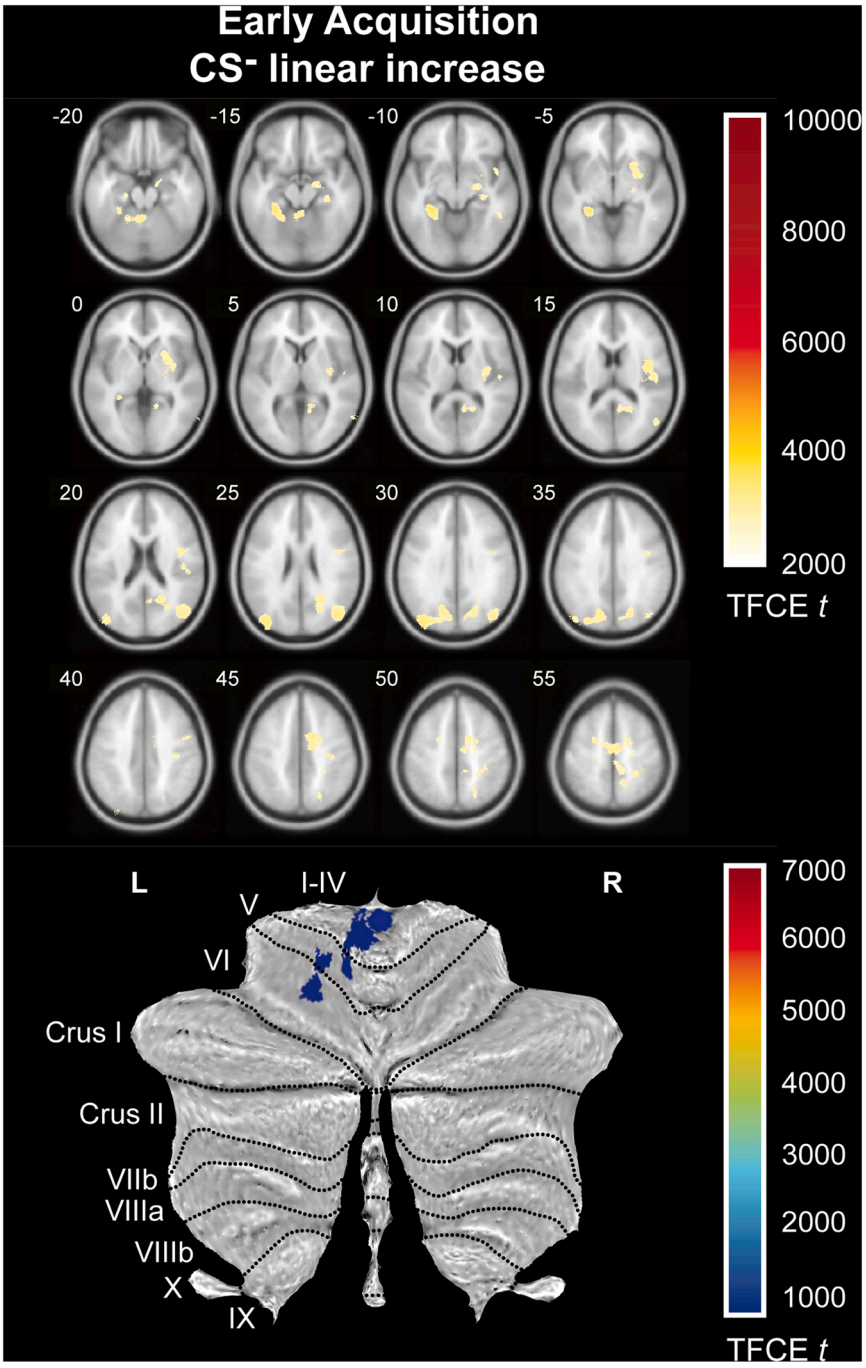

Fig. 4. CS-induced trial-by-trial changes in BOLD responses during early acquisition displayed separately for the cerebrum (upper panel) and cerebellum (lower panel). Analyses of one sample t-tests yielded for the CS^- during acquisition significantly increased neural activation in anterior and posterior insula, midcingulate cortex, precuneus, hippocampus, angular gyrus, supplementary motor area, paracentral lobule as well as cerebellar lobules I-IV, V and VI. Significant clusters in the cerebellum are based on the SUIT atlas introduced by [122] and are displayed on a surface-based flatmap of the cerebellum (http://www.diedrichsenlab.org/imaging/suit_flatmap.htm). All activation clusters are displayed at $p < .05$ familywise error rate (FWE) correction based on the Threshold-Free Cluster Enhancement (TFCE) statistic image.

learning in the anterior and posterior insula, midcingulate cortex, hippocampus, medial and inferior parietal lobule as well as cerebral and cerebellar somatomotor regions. This neural activation pattern partially overlaps with the networks identified across the whole acquisition phase, but also emphasizes the gradual evolvement of brain responses specifically in the anterior insula, hippocampus, precuneus, supplementary motor area and paracentral lobule. These results are well in line with our previous work demonstrating that in the context of visceral pain, initially neutral cues rapidly engage emotional arousal, homeostatic-afferent and cortical modulatory networks during early differential conditioning [12,14]. However, there was no evidence for dynamic temporal changes in response to the threat cue during acquisition or time-dependent mechanisms in response to either cue during extinction.

The formation of associations between stimuli and the expression of corresponding behaviors is a major aspect in classical conditioning. Learning to discriminate different stimuli is therefore a fundamental ability to direct behavior and, in terms of visceral pain, even critical for survival [72]. This form of discrimination learning during classical conditioning procedures is achieved through reinforcement of one stimulus (CS^+) with the US while the other stimulus (CS^-) is not reinforced. Based on these contingencies, participants learn to distinguish between cues predicting negative outcomes and safety cues predicting positive outcomes. Herein, the threat cue has been associated with the frequent occurrence of the US during acquisition and thus is a feature-positive stimulus, i.e., individuals learn better to detect the association between two stimuli than the absence of a stimulus [73,74]. During this learning course, negatively reinforced cues induce wider

Table 7
Trial-by-trial changes in differential BOLD responses during early acquisition vs. early extinction.

Location	k_E	x	y	z	TFCE	p_{FWE}	Network
CS^+ linear increase ACQ > EXT		No significant results					
CS^+ linear increase EXT > ACQ		No significant results					
CS^- linear increase ACQ > EXT							
Precuneus	10937	-10	-57	6	3040.28	.022	Visual
Posterior cingulate cortex		-12	-53	6	3025.52	.023	Default
Precuneus		9	-49	12	2949.25	.025	Default
Lingual gyrus		9	-52	4	2948.44	.025	Default
Lingual gyrus	4573	-25	-49	-9	2752.53	.032	Visual
Fusiform gyrus		-29	-41	-19	2721.98	.033	Visual
Middle occipital gyrus	570	-34	-83	27	2523.51	.044	Visual
CS^- linear increase EXT > ACQ		No significant results					

Results of paired t-tests assessing CS-induced differential neural activation during early acquisition versus early extinction. Peak activations in the cerebrum are given with MNI coordinates and the corresponding large-scale network according to [124]. Activation clusters are reported with cluster size kE after application of Threshold-Free Cluster Enhancement (TFCE) at $p < .05$ family-wise error (FWE) correction.

generalization curves and increase sensory thresholds that are needed to perceive non-aversive stimuli as different [75–77]. Specifically, visceral pain as a ubiquitous and uniquely aversive sensation is capable to readily induce strong and robust fear responses [12–14,16,19,32] that are perceived as more unpleasant and fear provoking compared to other pain modalities [45,47,56,78,79].

On the other hand, safety signals are feature-negative cues and thus probably take longer to learn than aversive, feature-positive cues as individuals experience difficulties in processing non-occurrences of stimuli, i.e., the absence of the US [80,81]. This type of learning may be accounted for by temporal difference algorithms where prediction errors are used as teaching signal to detect which stimuli are contingently followed by rewards, e.g. during avoidance behavior [82,83]. It has been assumed that these prediction errors may have characteristics of an attention signal reflecting the increased salience in response to the unexpected receipt and omission of reward [84,85]. Therefore, increasing demands for safety learning might be reflected by a stronger involvement of salience processing, allocation of attentional resources and the integration of multisensory information. First evidence in animals demonstrated that increased salience of the safety cue improves the exploration and discrimination of non-threatening stimuli, thereby decreasing fearful responses [86] while inhibition of basolateral amygdala neurons disrupts the maintenance of conditioned stimulus salience [87].

One brain region highly implicated in salience processing in humans is the anterior insula, serving to detect novel stimuli or salient events, to mediate interoceptive attention, and to coordinate cognitive, emotional and central-executive networks to guide behavior [88–91]. Specifically, during initial safety learning, when participants are presumably not fully aware about safety cue properties, increased salience and attention to physiological signals arising from the body may induce hypervigilance in order to prepare for potential imminent pain. This fits well with increased activation of the precuneus and hippocampus that were also part of the safety network identified by others [24]. The precuneus has been demonstrated to have distinct subdivisions encompassing sensorimotor, cognitive-associative and visual functions [92] and is known to implement a wide range of higher-order cognitive functions as well as to elaborate highly integrated and associative information [93]. Together with the anterior insula, the precuneus moreover forms a fronto-parietal attention circuit implicated in alertness, sustained attention and recollection [94,95]. Considerable evidence has indicated the hippocampus in the neural circuitry of fear conditioning as a key region supporting the acquisition, consolidation, retrieval and contextual modulation of fear [96,97] as well as the regulation of fear and avoidance [98,99]. Specifically, in interaction with the amygdala, the hippocampus is assumed to form declarative representations of stimuli with emotional significance [37,100].

The gradual evolvement of safety cue properties inevitably depends on the incremental capability of the threat cue in predicting imminent pain, both associative learning processes resulting from the difference between the expected and actual outcome. This prediction signal amplifies or attenuates expectations arising with CS appearance throughout consecutive trials of explicit and implicit cue-outcome presentations [101]. Opposed to instructed learning paradigms, our participants did not receive any information about CS-US contingencies, requiring them to learn trial by trial to differentiate between cues signaling imminent visceral pain and cues signaling the absence of pain. The neural activation pattern underlying the early time course of safety learning corresponds to a neuroimaging study demonstrating that the insula, supplementary motor and visual cortices mediate positive prediction signaling. For time-dependent changes in neural activation related to the CS^-, we observed an increased contribution of somatomotor cerebellar regions that might reflect anticipatory processes to prepare the organism for upcoming non-occurrence of aversive experiences and concomitant relaxation [102]. Time-dependent changes, however, only partly overlapped with cerebellar regions activated related to the CS- in early acquisition compared to rest. Reasons are unclear, and findings need to be verified in future studies.

While distinct neural processing of safety cues does not appear to be specific to pain-related conditioning [24], it may bear special relevance in chronic pain as a mechanism underlying maladaptive avoidance behavior, particularly regarding interoceptive, visceral pain [56]. In general, learned safety signals are adaptive, provide relief from fearful situations and foster inhibition of learned fear [23]. However, aberrant safety learning, behavior and deficient extinction constitute a clinically relevant phenotype in fear- and stress-related disorders including post-traumatic stress disorder [103,104] and depression [105,106]. Likewise, patients with disorders of the gut-brain axis like irritable bowel syndrome (IBS) demonstrate altered fear acquisition [20,107–111], fear extinction [20,22] and reactivation of visceral pain-related memories [20]. First evidence moreover indicates that IBS patients rate safety cues as more pleasant after acquisition, more accurately report safety cue contingency, and demonstrate increased neural activation in reward-related brain regions [20]. Through sustained hypervigilance, safety seeking becomes maladaptive and constitutes one key component in pain-related avoidance behavior [112], calling for future studies addressing avoidance behavior rather than fear reduction to advance treatment approaches in chronic pain [113]. Cognitive behavioral therapy (CBT) has been shown to effectively address the evaluation and modification of IBS patients' thoughts and behavior by remediating maladaptive affective-cognitive processes [114–117]. Specifically, exposure techniques as one component of CBT are reported to alleviate symptom-related anxiety and symptom severity by challenging patients to gradually face situations they commonly avoid [118], to incorporate behavior that likely triggers gastrointestinal symptoms [119] or to assess their safety behaviors [120]. Through targeted interventions, patients can therefore benefit from the therapeutic effects of extinction learning to reduce fear and maladaptive emotions and cognitions. Despite their clinical relevance and documented efficacy, however, little is known about the processes by which cognitive behavioral therapies like exposure achieve their effects. Based on first experimental evidence in healthy individuals on visceral pain-related fear and safety acquisition and extinction, as for example reported herein, further studies are needed to unravel the behavioral and neural mechanisms of the gut-brain axis relevant to these behavioral treatment approaches [121].

Funding

This project was funded by the Deutsche Forschungsgemeinschaft (German Research Foundation), project number 316803389, SFB 1280, subprojects F02, A10 and A12. The funding agency had no role in the conception, analysis or interpretation of the data.

CRediT authorship contribution statement

FL, TME and TS analyzed the data; FL, TME, TS, NA, CAG, HHQ, SE and DT interpreted the results of the analyses; FL, TME and TS prepared the figures; FL, TS and DT drafted the manuscript; FL, TME, TS, NA, CAG, HHQ, SE and DT edited and revised the manuscript; FL, TME, TS, NA, CAG, HHQ, SE and DT approved the final version of the manuscript.

Conflict of interest statement

The authors have no conflicts of interest to declare.

References

[1] J.F. Cryan, K.J. O'riordan, C.S.M. Cowan, K.V. Sandhu, T.F.S. Bastiaanssen, M. Boehme, et al., The microbiota-gut-brain axis, Physiol. Rev. 99 (2019) 1877–2013, https://doi.org/10.1152/physrev.00018.2018.
[2] E.A. Mayer, Gut feelings: The emerging biology of gut-"brain communication, Nat. Rev. Neurosci. 12 (2011) 453–466, https://doi.org/10.1038/nrn3071.
[3] Y. Lee, Y.K. Kim, Understanding the connection between the gut–brain axis and stress/anxiety disorders, Curr. Psychiatry Rep. 23 (2021), https://doi.org/10.1007/s11920-021-01235-x.
[4] E.A. Mayer, J.S. Labus, K. Tillisch, S.W. Cole, P. Baldi, Towards a systems view of IBS, Nat. Rev. Gastroenterol. Hepatol. 12 (2015) 1–14, https://doi.org/10.1038/nrgastro.2015.121.
[5] L.H. Morais, H.L. Schreiber, S.K. Mazmanian, The gut microbiota–brain axis in behaviour and brain disorders, Nat. Rev. Microbiol. (2020), https://doi.org/10.1038/s41579-020-00460-0.
[6] N. Weltens, J. Iven, L. Van Oudenhove, M. Kano, The gut–brain axis in health neuroscience: implications for functional gastrointestinal disorders and appetite regulation, Ann. N. Y. Acad. Sci. 1428 (2018) 129–150, https://doi.org/10.1111/nyas.13969.
[7] A. Craig, How do you feel? Interoception: The sense of the physiological condition of the body, Nat. Rev. Neurosci. 3 (2002) 655–666, https://doi.org/10.1038/nrn894.
[8] L. Quadt, H.D. Critchley, S.N. Garfinkel, The neurobiology of interoception in health and disease, Ann. N. Y. Acad. Sci. 1428 (2018) 112–128, https://doi.org/10.1111/nyas.13915.
[9] H.D. Critchley, Neural mechanisms of autonomic, affective, and cognitive integration, J. Comp. Neurol. 493 (2005) 154–166, https://doi.org/10.1002/cne.20749.
[10] K.S. Quigley, S. Kanoski, W.M. Grill, L.F. Barrett, M. Tsakiris, Functions of interoception: From energy regulation to experience of the self, Trends Neurosci. 44 (2021) 29–38, https://doi.org/10.1016/j.tins.2020.09.008.
[11] H.D. Critchley, S.N. Garfinkel, Interoception and emotion, Curr. Opin. Psychol. 17 (2017) 7–14, https://doi.org/10.1016/j.copsyc.2017.04.020.
[12] A. Icenhour, J. Kattoor, S. Benson, A. Boekstegers, M. Schlamann, C.J. Merz, et al., Neural circuitry underlying effects of context on human pain-related fear extinction in a renewal paradigm, Hum. Brain Mapp. 36 (2015) 3179–3193, https://doi.org/10.1002/hbm.22837.
[13] J. Kattoor, E.R. Gizewski, V. Kotsis, S. Benson, C. Gramsch, N. Theysohn, et al., Fear conditioning in an abdominal pain model: Neural responses during associative learning and extinction in healthy subjects, PLoS One 8 (2013), e51149, https://doi.org/10.1371/journal.pone.0051149.
[14] F. Labrenz, A. Icenhour, M. Schlamann, M. Forsting, U. Bingel, S. Elsenbruch, From Pavlov to pain: How predictability affects the anticipation and processing of visceral pain in a fear conditioning paradigm, Neuroimage 130 (2016) 104–114, https://doi.org/10.1016/j.neuroimage.2016.01.064.
[15] E. Ceunen, J. Zaman, N. Weltens, E. Sarafanova, V. Arijs, J.W.S. Vlaeyen, et al., Learned fear of gastrointestinal sensations in healthy adults, Clin. Gastroenterol. Hepatol. 14 (2016) 1552–1558, https://doi.org/10.1016/j.cgh.2016.04.035.
[16] A. Icenhour, F. Labrenz, C. Ritter, N. Theysohn, M. Forsting, U. Bingel, et al., Learning by experience? Visceral pain-related neural and behavioral responses in a classical conditioning paradigm, Neurogastroenterol. Motil. 29 (2017), e13026, https://doi.org/10.1111/nmo.13026.
[17] J. Zaman, N. Weltens, H.G. Ly, D. Struyf, J.W.S. Vlaeyen, O. Van den Bergh, et al., Influence of interoceptive fear learning on visceral perception, Psychosom. Med. 78 (2016) 1–11, https://doi.org/10.1097/PSY.0000000000000257.
[18] J. Zaman, V.J. Madden, J. Iven, K. Wiech, N. Weltens, H.G. Ly, et al., Biased intensity judgements of visceral sensations after learning to fear visceral stimuli: A drift diffusion approach, J. Pain. 18 (2017) 1197–1208, https://doi.org/10.1016/j.jpain.2017.04.011.
[19] A. Icenhour, L. Petrakova, N. Hazzan, N. Theysohn, C.J. Merz, S. Elsenbruch, When gut feelings teach the brain to fear pain: Context-dependent activation of the central fear network in a novel interoceptive conditioning paradigm, Neuroimage 238 (2021), 118229, https://doi.org/10.1016/j.neuroimage.2021.118229.
[20] A. Icenhour, J. Langhorst, S. Benson, M. Schlamann, S. Hampel, H. Engler, et al., Neural circuitry of abdominal pain-related fear learning and reinstatement in irritable bowel syndrome, Neurogastroenterol. Motil. 27 (2015) 114–127, https://doi.org/10.1111/nmo.12489.
[21] F. Labrenz, K. Wrede, M. Forsting, H. Engler, M. Schedlowski, S. Elsenbruch, et al., Alterations in functional connectivity of resting state networks during experimental endotoxemia - An exploratory study in healthy men, Brain Behav. Immun. 54 (2016) 17–26, https://doi.org/10.1016/j.bbi.2015.11.010.
[22] J.S. Labus, C.S. Hubbard, J. Bueller, B. Ebrat, K. Tillisch, M. Chen, et al., Impaired emotional learning and involvement of the corticotropin-releasing factor signaling system in patients with irritable bowel syndrome, Gastroenterology 145 (2013) 1253–1261, https://doi.org/10.1053/j.gastro.2013.08.016.
[23] J.P. Christianson, A.B.P. Fernando, A.M. Kazama, T. Jovanovic, L.E. Ostroff, S. Sangha, Inhibition of fear by learned safety signals: A mini-symposium review, J. Neurosci. 32 (2012) 14118–14124, https://doi.org/10.1523/JNEUROSCI.3340-12.2012.
[24] M.A. Fullana, B.J. Harrison, C. Soriano-Mas, B. Vervliet, N. Cardoner, A. Àvila-Parcet, et al., Neural signatures of human fear conditioning: An updated and extended meta-analysis of fMRI studies, Mol. Psychiatry 21 (2016) 500–508, https://doi.org/10.1038/mp.2015.88.
[25] E. Kong, F.J. Monje, J. Hirsch, D.D. Pollak, Learning not to fear: Neural correlates of learned safety, Neuropsychopharmacology 39 (2014) 515–527, https://doi.org/10.1038/npp.2013.191.
[26] F. Labrenz, A. Icenhour, M. Thürling, M. Schlamann, M. Forsting, D. Timmann, et al., Sex differences in cerebellar mechanisms involved in pain-related safety learning, Neurobiol. Learn. Mem. 123 (2015) 92–99, https://doi.org/10.1016/j.nlm.2015.05.006.
[27] J. Kattoor, M. Thürling, E.R. Gizewski, M. Forsting, D. Timmann, S. Elsenbruch, Cerebellar contributions to different phases of visceral aversive extinction learning, Cerebellum 13 (2014) 1–8, https://doi.org/10.1007/s12311-013-0512-9.
[28] R.A. Rescorla, A.R. Wagner, A theory of Pavlovian conditioning: Variations in the effectiveness of reinforcement and nonreinforcement Human Learning View project Taste Aversion Learning View project, Class. Cond. II Curr. Res. Theory (1972) 64–99. ⟨https://www.researchgate.net/publication/233820243⟩.
[29] J.M. Pearce, G. Hall, A model for Pavlovian learning: Variations in the effectiveness of conditioned but not of unconditioned stimuli, Psychol. Rev. 87 (1980) 532–552, https://doi.org/10.1037/0033-295X.87.6.532.
[30] S. Maren, Neurobiology of Pavlovian fear conditioning, Annu. Rev. Neurosci. 24 (2001) 897–931, https://doi.org/10.1146/annurev.neuro.24.1.897.
[31] A. Öhman, A. Eriksson, C. Olofsson, One-trial learning and superior resistance to extinction of autonomic responses conditioned to potentially phobic stimuli, J. Comp. Physiol. Psychol. 88 (1975) 619–627, https://doi.org/10.1037/h0078388.
[32] C. Gramsch, J. Kattoor, A. Icenhour, M. Forsting, M. Schedlowski, E.R. Gizewski, et al., Learning pain-related fear: Neural mechanisms mediating rapid differential conditioning, extinction and reinstatement processes in human visceral pain, Neurobiol. Learn. Mem. 116 (2014) 36–45, https://doi.org/10.1016/j.nlm.2014.08.003.
[33] L. Yágüez, S. Coen, L.J. Gregory, E. Amaro, C. Altman, M.J. Brammer, et al., Brain response to visceral aversive conditioning: A functional magnetic resonance imaging study, Gastroenterology 128 (2005) 1819–1829, https://doi.org/10.1053/j.gastro.2005.02.068.
[34] U. Stockhorst, P. Enck, S. Klosterhalfen, Role of classical conditioning in learning gastrointestinal symptoms, World J. Gastroenterol. 13 (2007) 3430–3437, https://doi.org/10.3748/wjg.v13.i25.3430.
[35] C. Mediavilla, F. Molina, A. Puerto, Concurrent conditioned taste aversion: A learning mechanism based on rapid neural versus flexible humoral processing of visceral noxious substances, Neurosci. Biobehav. Rev. 29 (2005) 1107–1118, https://doi.org/10.1016/j.neubiorev.2005.06.002.
[36] H. Welzl, P. D'Adamo, H.-P. Lipp, Conditioned taste aversion as a learning and memory paradigm, Behav. Brain Res. 125 (2001) 205–213, https://doi.org/10.1016/S0166-4328(01)00302-3.
[37] E.A. Phelps, M.R. Delgado, K.I. Nearing, J.E. Ledoux, Extinction learning in humans: Role of the amygdala and vmPFC, Neuron 43 (2004) 897–905, https://doi.org/10.1016/j.neuron.2004.08.042.
[38] D.C. Knight, C.D. T, C.N. Smith, E.A. Stein, F.J. Helmstetter, Neural substrates mediating human delay and trace fear conditioning, J. Neurosci. 24 (2004) 218–228, https://doi.org/10.1523/JNEUROSCI.0433-03.2004.
[39] C. Büchel, J. Morris, R.J. Dolan, K.J. Friston, Brain systems mediating aversive conditioning: An event-related fMRI study, Neuron 20 (1998) 947–957, https://doi.org/10.1016/S0896-6273(00)80476-6.
[40] K.S. Labar, J.C. Gatenby, J.C. Gore, J.E. Ledoux, E.A. Phelps, Human amygdala activation during conditioned fear acquisition and extinction: A mixed-trial fMRI study to investigate amygdala function in human populations have produced inconsistent results across techniques. Whereas neuropsychological studies have repo, Neuron 20 (1998) 937–945.
[41] J.S. Morris, C. Büchel, R.J. Dolan, Parallel neural responses in amygdala subregions and sensory cortex during implicit fear conditioning, Neuroimage 13 (2001) 1044–1052, https://doi.org/10.1006/nimg.2000.0721.

[42] H.D. Critchley, C.J. Mathias, R.J. Dolan, Fear conditioning in humans: The influence of awareness and autonomic arousal on functional neuroanatomy, Neuron 33 (2002) 653–663, https://doi.org/10.1016/S0896-6273(02)00588-3.

[43] D.C. Knight, C.N. Smith, D.T. Cheng, E.A. Stein, F.J. Helmstetter, Amygdala and hippocampal activity during acquisition and extinction of human fear conditioning, Cogn. Affect. Behav. Neurosci. 4 (2004) 317–325, https://doi.org/10.3758/CABN.4.3.317.

[44] C.J. Merz, A. Hermann, R. Stark, O.T. Wolf, Cortisol modifies extinction learning of recently acquired fear in men, Soc. Cogn. Affect. Neurosci. 9 (2013) 1426–1434, https://doi.org/10.1093/scan/nst137.

[45] L.R. Koenen, R.J. Pawlik, A. Icenhour, L. Petrakova, K. Forkmann, N. Theysohn, et al., Associative learning and extinction of conditioned threat predictors across sensory modalities, Commun. Biol. 4 (2021) 1–17, https://doi.org/10.1038/s42003-021-02008-1.

[46] T.B. Lonsdorf, M.M. Menz, M. Andreatta, M.A. Fullana, A. Golkar, J. Haaker, et al., Don't fear 'fear conditioning': Methodological considerations for the design and analysis of studies on human fear acquisition, extinction, and return of fear, Neurosci. Biobehav. Rev. 77 (2017) 247–285, https://doi.org/10.1016/j.neubiorev.2017.02.026.

[47] L.R. Koenen, A. Icenhour, K. Forkmann, A. Pasler, N. Theysohn, M. Forsting, et al., Greater fear of visceral pain contributes to differences between visceral and somatic pain in healthy women, Pain 158 (2017) 1599–1608, https://doi.org/10.1097/j.pain.0000000000000924.

[48] B. Sacchetti, B. Scelfo, P. Strata, Cerebellum and emotional behavior, Neuroscience 162 (2009) 756–762, https://doi.org/10.1016/j.neuroscience.2009.01.064.

[49] P. Strata, The emotional cerebellum, Cerebellum 14 (2015) 570–577, https://doi.org/10.1007/s12311-015-0649-9.

[50] D. Timmann, J. Drepper, M. Frings, M. Maschke, S. Richter, M. Gerwig, et al., The human cerebellum contributes to motor, emotional and cognitive associative learning. A review, Cortex 46 (2010) 845–857, https://doi.org/10.1016/j.cortex.2009.06.009.

[51] C. Bellebaum, I. Daum, Mechanisms of cerebellar involvement in associative learning, Cortex 47 (2011) 128–136, https://doi.org/10.1016/j.cortex.2009.07.016.

[52] I. Lange, Z. Kasanova, L. Goossens, N. Leibold, C.I. De Zeeuw, T. van Amelsvoort, et al., The anatomy of fear learning in the cerebellum: A systematic meta-analysis, Neurosci. Biobehav. Rev. 59 (2015) 83–91, https://doi.org/10.1016/j.neubiorev.2015.09.019.

[53] K.S. LaBar, J.C. Gatenby, J.C. Gore, J.E. LeDoux, E.A. Phelps, Human amygdala activation during conditioned fear acquisition and extinction: A mixed-trial fMRI study, Neuron 20 (1998) 937–945. ⟨http://ir.library.oregonstate.edu/xmlui/bitstream/handle/1957/55926/Berzins_MPP_Essay.pdf;jsessionid=5F5C2F1509C96944F8A639EB4295CB99?sequence=1⟩.

[54] T. Beckers, A.-M. Krypotos, Y. Boddez, M. Effting, M. Kindt, What's wrong with fear conditioning? Biol. Psychol. 92 (2013) 90–96, https://doi.org/10.1016/j.biopsycho.2011.12.015.

[55] K.M. Ryan, M.J. Zimmer-Gembeck, D.L. Neumann, A.M. Waters, The need for standards in the design of differential fear conditioning and extinction experiments in youth: A systematic review and recommendations for research on anxiety, Behav. Res. Ther. 112 (2019) 42–62, https://doi.org/10.1016/j.brat.2018.11.009.

[56] L.R. Koenen, A. Icenhour, K. Forkmann, N. Theysohn, M. Forsting, U. Bingel, et al., From anticipation to the experience of pain: The importance of visceral versus somatic pain modality in neural and behavioral responses to pain-predictive cues, Psychosom. Med. 80 (2018) 826–835, https://doi.org/10.1097/PSY.0000000000000612.

[57] J.A. Greco, I. Liberzon, Neuroimaging of fear-associated learning, Neuropsychopharmacology 41 (2016) 320–334, https://doi.org/10.1038/npp.2015.255.

[58] T.M. Ernst, A.E. Brol, M. Gratz, C. Ritter, U. Bingel, M. Schlamann, et al., The cerebellum is involved in processing of predictions and prediction errors in a fear conditioning paradigm, Elife 8 (2019) 1–26, https://doi.org/10.7554/eLife.46831.

[59] R. Apps, P. Strata, Neuronal circuits for fear and anxiety — the missing link, Nat. Rev. Neurosci. 16 (2015) 642, https://doi.org/10.1038/nrn4028.

[60] X. Guell, J.D.E. Gabrieli, J.D. Schmahmann, Triple representation of language, working memory, social and emotion processing in the cerebellum: Convergent evidence from task and seed-based resting-state fMRI analyses in a single large cohort, Neuroimage 172 (2018) 437–449, https://doi.org/10.1016/j.neuroimage.2018.01.082.

[61] C.J. Stoodley, J.D. Schmahmann. Functional Topography of the Human Cerebellum, first ed., Elsevier B.V, 2018 https://doi.org/10.1016/B978-0-444-63956-1.00004-7.

[62] M.L. Seghier, The angular gyrus: Multiple functions and multiple subdivisions, Neuroscientist 19 (2013) 43–61, https://doi.org/10.1177/1073858412440596.

[63] B.E. Depue, T. Curran, M.T. Banich, Prefrontal regions orchestrate suppression of emotional memories via a two-phase process, Sci. (80). 317 (2007) 215–219, https://doi.org/10.1126/science.1139560.

[64] K.N. Ochsner, J.J. Gross, The cognitive control of emotion, Trends Cogn. Sci. 9 (2005) 242–249, https://doi.org/10.1016/j.tics.2005.03.010.

[65] K.N. Ochsner, J.A. Silvers, J.T. Buhle, Review and evolving model of the cognitive control of emotion, Ann. N. Y. Acad. Sci. (2012) E1–E24, https://doi.org/10.1111/j.1749-6632.2012.06751.x.Functional.

[66] Y. Shiba, A.M. Santangelo, A.C. Roberts, Beyond the medial regions of prefrontal cortex in the regulation of fear and anxiety, Front. Syst. Neurosci. 10 (2016) 1–13, https://doi.org/10.3389/fnsys.2016.00012.

[67] A. Zilverstand, M.A. Parvaz, R.Z. Goldstein, Neuroimaging cognitive reappraisal in clinical populations to define neural targets for enhancing emotion regulation. A systematic review, Neuroimage 151 (2017) 105–116, https://doi.org/10.1016/j.neuroimage.2016.06.009.

[68] F. Eippert, R. Veit, N. Weiskopf, M. Erb, N. Birbaumer, S. Anders, Regulation of emotional responses elicited by threat-related stimuli, Hum. Brain Mapp. 28 (2007) 409–423, https://doi.org/10.1002/hbm.20291.

[69] A. Etkin, T. Egner, R. Kalisch, Emotional processing in anterior cingulate and medial prefrontal cortex, Trends Cogn. Sci. 15 (2011) 85–93, https://doi.org/10.1016/j.tics.2010.11.004.

[70] M.L. Mechias, A. Etkin, R. Kalisch, A meta-analysis of instructed fear studies: Implications for conscious appraisal of threat, Neuroimage 49 (2010) 1760–1768, https://doi.org/10.1016/j.neuroimage.2009.09.040.

[71] M.R. Gilmartin, N.L. Balderston, F.J. Helmstetter, Prefrontal cortical regulation of fear learning, Trends Neurosci. 37 (2014) 455–464, https://doi.org/10.1016/j.tins.2014.05.004.

[72] H. Jenkins, R. Sainsbury, The development of stimulus control through differential reinforcement, in: N.J. Mackintosh, W.K. Honig (Eds.), Fundam. Issues Assoc. Learn., Dalhousie University Press, Halifax, NS, 1969, pp. 123–161.

[73] M.E. Bouton, J.B. Nelson, Mechanisms of feature-positive and feature-negative discrimination learning in an appetitive conditioning paradigm. Occas. Setting Assoc. Learn. Cogn. Anim, American Psychological Association, Washington, DC, US, 1998, pp. 69–112, https://doi.org/10.1037/10298-003.

[74] P.C. Holland, Temporal determinants of occasion setting in feature-positive discriminations, Anim. Learn. Behav. 14 (1986) 111–120, https://doi.org/10.3758/BF03200045.

[75] J. Resnik, N. Sobel, R. Paz, Auditory aversive learning increases discrimination thresholds, Nat. Neurosci. 14 (2011) 791–796, https://doi.org/10.1038/nn.2802.

[76] E. Schechtman, O. Laufer, R. Paz, Negative valence widens generalization of learning, J. Neurosci. 30 (2010) 10460–10464, https://doi.org/10.1523/JNEUROSCI.2377-10.2010.

[77] L. Shalev, R. Paz, G. Avidan, Visual aversive learning compromises sensory discrimination, J. Neurosci. 38 (2018) 2766–2779, https://doi.org/10.1523/JNEUROSCI.0889-17.2017.

[78] P. Dunckley, R.G. Wise, Q. Aziz, D. Painter, J. Brooks, I. Tracey, et al., Cortical processing of visceral and somatic stimulation: Differentiating pain intensity from unpleasantness, Neuroscience 133 (2005) 533–542, https://doi.org/10.1016/j.neuroscience.2005.02.041.

[79] S. Benson, C. Siebert, L.R. Koenen, H. Engler, J. Kleine-Borgmann, U. Bingel, et al., Cortisol affects pain sensitivity and pain-related emotional learning in experimental visceral but not somatic pain: a randomized controlled study in healthy men and women, Pain 160 (2019) 1719–1728, https://doi.org/10.1097/j.pain.0000000000001579.

[80] C.R. Crowell, T.P. Bernhardt, The feature-positive effect and sign-tracking behavior during discrimination learning in the rat, Anim. Learn. Behav. 7 (1979) 313–317, https://doi.org/10.3758/BF03209675.

[81] R.S. Sainsbury, H.M. Jenkins, Feature-positive effect in discrimination learning, Proc. Annu. Conv. Am. Psychol. 2 (1967) 17–118.

[82] M. Moutoussis, R.P. Bentall, J. Williams, P. Dayan, A temporal difference account of avoidance learning, Netw. Comput. Neural Syst. 19 (2008) 137–160, https://doi.org/10.1080/09548980802192784.

[83] B. Vervliet, I. Lange, M.R. Milad, Temporal dynamics of relief in avoidance conditioning and fear extinction: Experimental validation and clinical relevance, Behav. Res. Ther. 96 (2017) 66–78, https://doi.org/10.1016/j.brat.2017.04.011.

[84] J.P. O'Doherty, P. Dayan, K. Friston, H. Critchley, R.J. Dolan, Temporal difference models and reward-related learning in the human brain, Neuron 38 (2003) 329–337, https://doi.org/10.1016/S0896-6273(03)00169-7.

[85] P. Dayan, S. Kakade, P.R. Montague, Learning and selective attention, Nat. Neurosci. 3 (2000) 1218–1223, https://doi.org/10.1038/81504.

[86] I. Nahmoud, J.G. Vasquez, H. Cho, T. Dennis-Tiwary, E. Likhtik, Salient safety conditioning improves novel discrimination learning, Behav. Brain Res. 397 (2021), 112907, https://doi.org/10.1016/j.bbr.2020.112907.

[87] A. Sengupta, J.O.Y. Yau, P. Jean-Richard-Dit-Bressel, Y. Liu, E.Z. Millan, J. M. Power, et al., Basolateral amygdala neurons maintain aversive emotional salience, J. Neurosci. 38 (2018) 3001–3012, https://doi.org/10.1523/JNEUROSCI.2460-17.2017.

[88] A. Craig, How do you feel - now? The anterior insula and human awareness, Nat. Rev. Neurosci. 10 (2009) 59–70, https://doi.org/10.1038/nrn2555.

[89] V. Menon, L.Q. Uddin, Saliency, switching, attention and control: A network model of insula function, Brain Struct. Funct. 214 (2010) 655–667, https://doi.org/10.1007/s00429-010-0262-0.

[90] W.W. Seeley, V. Menon, A.F. Schatzberg, J. Keller, G.H. Glover, H. Kenna, et al., Dissociable intrinsic connectivity networks for salience processing and executive control, J. Neurosci. 27 (2007) 2349–2356, https://doi.org/10.1523/JNEUROSCI.5587-06.2007.

[91] K. Wiech, C.-s Lin, K.H. Brodersen, U. Bingel, M. Ploner, I. Tracey, Anterior Insula Integrates Information about salience into perceptual decisions about pain, J. Neurosci. 30 (2010) 16324–16331, https://doi.org/10.1523/JNEUROSCI.2087-10.2010.

[92] D.S. Margulies, J.L. Vincent, C. Kelly, G. Lohmann, L.Q. Uddin, B.B. Biswal, et al., Precuneus shares intrinsic functional architecture in humans and monkeys, Proc. Natl. Acad. Sci. 106 (2009) 20069–20074, https://doi.org/10.1073/pnas.0905314106.

[93] A.E. Cavanna, M.R. Trimble, The precuneus: A review of its functional anatomy and behavioural correlates, Brain 129 (2006) 564–583, https://doi.org/10.1093/brain/awl004.
[94] A. Fornito, B.J. Harrison, A. Zalesky, J.S. Simons, Competitive and cooperative dynamics of large-scale brain functional networks supporting recollection, Proc. Natl. Acad. Sci. U. S. A. 109 (2012) 12788–12793, https://doi.org/10.1073/pnas.1204185109.
[95] E.M. Gordon, T.O. Laumann, B. Adeyemo, J.F. Huckins, W.M. Kelley, S. E. Petersen, Generation and evaluation of a cortical area parcellation from resting-state correlations, Cereb. Cortex. 26 (2016) 288–303, https://doi.org/10.1093/cercor/bhu239.
[96] F. Sotres-Bayon, C.K. Cain, J.E. LeDoux, Brain mechanisms of fear extinction: Historical perspectives on the contribution of prefrontal cortex, Biol. Psychiatry 60 (2006) 329–336, https://doi.org/10.1016/j.biopsych.2005.10.012.
[97] G.J. Quirk, D. Mueller, Neural mechanisms of extinction learning and retrieval, Neuropsychopharmacology 33 (2008) 56–72, https://doi.org/10.1038/sj.npp.1301555.
[98] C.A. Hartley, E.A. Phelps, Changing fear: The neurocircuitry of emotion regulation, Neuropsychopharmacology 35 (2010) 136–146, https://doi.org/10.1038/npp.2009.121.
[99] J.M. Moscarello, S. Maren, Flexibility in the face of fear: hippocampal–prefrontal regulation of fear and avoidance, Curr. Opin. Behav. Sci. 19 (2018) 44–49, https://doi.org/10.1016/j.cobeha.2017.09.010.
[100] M.P. Richardson, B.A. Strange, R.J. Dolan, Encoding of emotional memories depends on amygdala and hippocampus and their interactions, Nat. Neurosci. 7 (2004) 278–285, https://doi.org/10.1038/nn1190.
[101] S.S.Y. Li, G.P. McNally, The conditions that promote fear learning: Prediction error and Pavlovian fear conditioning, Neurobiol. Learn. Mem. 108 (2014) 14–21, https://doi.org/10.1016/j.nlm.2013.05.002.
[102] L.F. Koziol, D. Budding, N. Andreasen, S. D'Arrigo, S. Bulgheroni, H. Imamizu, et al., Consensus paper: The cerebellum's role in movement and cognition, Cerebellum 13 (2014) 151–177, https://doi.org/10.1007/s12311-013-0511-x.
[103] T. Jovanovic, A. Kazama, J. Bachevalier, M. Davis, Impaired safety signal learning may be a biomarker of PTSD, Neuropharmacology 62 (2012) 695–704, https://doi.org/10.1016/j.neuropharm.2011.02.023.
[104] L.D. Straus, S.P.A. Drummond, V.B. Risbrough, S.B. Norman, Sleep disruption, safety learning, and fear extinction in humans: implications for posttraumatic stress disorder, Curr. Top. Behav. Neurosci., Ger. (2017) 193–205, https://doi.org/10.1007/7854_2017_31.
[105] J.M. Newby, M.L. Moulds, Negative intrusive memories in depression: The role of maladaptive appraisals and safety behaviours, J. Affect. Disord. 126 (2010) 147–154, https://doi.org/10.1016/j.jad.2010.03.012.
[106] M.L. Moulds, E. Kandris, A.D. Williams, T.J. Lang, The use of safety behaviours to manage intrusive memories in depression, Behav. Res. Ther. 46 (2008) 573–580, https://doi.org/10.1016/j.brat.2008.02.001.
[107] S.M. Berman, B.D. Naliboff, B. Suyenobu, J.S. Labus, J. Stains, G. Ohning, et al., Reduced brainstem inhibition during anticipated pelvic visceral pain correlates with enhanced brain response to the visceral stimulus in women with irritable bowel syndrome, J. Neurosci. 28 (2008) 349–359, https://doi.org/10.1523/JNEUROSCI.2500-07.2008.
[108] J. Claassen, F. Labrenz, T.M. Ernst, A. Icenhour, J. Langhorst, M. Forsting, et al., Altered cerebellar activity in visceral pain-related fear conditioning in irritable bowel syndrome, Cerebellum 16 (2017) 508–517, https://doi.org/10.1007/s12311-016-0832-7.
[109] J.-Y. Hong, B.D. Naliboff, J.S. Labus, A. Gupta, L.A. Kilpatrick, C. Ashe-Mcnalley, et al., Altered brain responses in subjects with irritable bowel syndrome during cued and uncued pain expectation, Neurogastroenterol. Motil. 28 (2016) 127–138, https://doi.org/10.1111/nmo.12710.
[110] B.D. Naliboff, A.M. Waters, J.S. Labus, L. Kilpatrick, M.G. Craske, L. Chang, et al., Increased acoustic startle responses in IBS patients during abdominal and nonabdominal threat, Psychosom. Med 70 (2008) 920–927, https://doi.org/10.1097/PSY.0b013e318186d858.
[111] B.D. Naliboff, S. Berman, B. Suyenobu, J.S. Labus, L. Chang, J. Stains, et al., Longitudinal change in perceptual and brain activation response to visceral stimuli in irritable bowel syndrome patients, Gastroenterology 131 (2006) 352–365, https://doi.org/10.1053/j.gastro.2006.05.014.
[112] J.W.S. Vlaeyen, G. Crombez, S.J. Linton, The fear-avoidance model of pain, Pain 157 (2016) 1588–1589, https://doi.org/10.1097/j.pain.0000000000000574.
[113] A. Meulders, Fear in the context of pain: Lessons learned from 100 years of fear conditioning research, Behav. Res. Ther. 131 (2020), 103635, https://doi.org/10.1016/j.brat.2020.103635.
[114] A.C. Ford, E.M.M. Quigley, B.E. Lacy, A.J. Lembo, Y.A. Saito, L.R. Schiller, et al., Effect of antidepressants and psychological therapies, including hypnotherapy, in irritable bowel syndrome: Systematic review and meta-analysis, Am. J. Gastroenterol. 109 (2014) 1350–1365, https://doi.org/10.1038/ajg.2014.148.
[115] J.M. Lackner, C. Mesmer, S. Morley, C. Dowzer, S. Hamilton, Psychological treatments for irritable bowel syndrome: A systematic review and meta-analysis, J. Consult. Clin. Psychol. 72 (2004) 1100–1113, https://doi.org/10.1037/0022-006X.72.6.1100.
[116] K.T. Laird, E.E. Tanner-Smith, A.C. Russell, S.D. Hollon, L.S. Walker, Short-term and long-term efficacy of psychological therapies for irritable bowel syndrome: A systematic review and meta-analysis, Clin. Gastroenterol. Hepatol. 14 (2016) 937–947, https://doi.org/10.1016/j.cgh.2015.11.020.
[117] K. Shah, M. Ramos-Garcia, J. Bhavsar, P. Lehrer, Mind-body treatments of irritable bowel syndrome symptoms: An updated meta-analysis, Behav. Res. Ther. 128 (2020), 103462, https://doi.org/10.1016/j.brat.2019.103462.
[118] H. Hesser, E. Hedman-Lagerlöf, E. Andersson, P. Lindfors, B. Ljótsson, How does exposure therapy work? A comparison between generic and gastrointestinal anxiety–specific mediators in a dismantling study of exposure therapy for irritable bowel syndrome, J. Consult. Clin. Psychol. 86 (2018) 254–267, https://doi.org/10.1037/ccp0000273.
[119] M.G. Craske, K.B. Wolitzky-Taylor, J. Labus, S. Wu, M. Frese, E.A. Mayer, et al., A cognitive-behavioral treatment for irritable bowel syndrome using interoceptive exposure to visceral sensations, Behav. Res. Ther. 49 (2011) 413–421, https://doi.org/10.1016/j.brat.2011.04.001.
[120] S. Windgassen, R. Moss-Morris, K. Goldsmith, T. Chalder, Key mechanisms of cognitive behavioural therapy in irritable bowel syndrome: The importance of gastrointestinal related cognitions, behaviours and general anxiety, J. Psychosom. Res. 118 (2019) 73–82, https://doi.org/10.1016/j.jpsychores.2018.11.013.
[121] L. Keefer, S.K. Ballou, D.A. Drossman, G. Ringstrom, S. Elsenbruch, B. Ljótsson, A rome working team report on brain-gut behavior therapies for disorders of gut-brain interaction, Gastroenterology (2021), https://doi.org/10.1053/j.gastro.2021.09.015.
[122] J. Diedrichsen, A spatially unbiased atlas template of the human cerebellum, Neuroimage 33 (2006) 127–138, https://doi.org/10.1016/j.neuroimage.2006.05.056.
[123] R.L. Buckner, F.M. Krienen, A. Castellanos, J.C. Diaz, B.T.T. Yeo, The organization of the human cerebellum estimated by intrinsic functional connectivity, J. Neurophysiol. 106 (2011) 2322–2345, https://doi.org/10.1152/jn.00339.2011.
[124] B.T. Thomas Yeo, F.M. Krienen, J. Sepulcre, M.R. Sabuncu, D. Lashkari, M. Hollinshead, et al., The organization of the human cerebral cortex estimated by intrinsic functional connectivity, J. Neurophysiol. 106 (2011) 1125–1165, https://doi.org/10.1152/jn.00338.2011.